CSIRO PUBLISHING

*International Journal of Wildland Fire* **2022**, *31*, 24–45
https://doi.org/10.1071/WF20126

# Application of compositional data analysis to determine the effects of heating mode, moisture status and plant species on pyrolysates

*David R. Weise* [A,D], *Thomas H. Fletcher* [B], *Mohammad-Saeed Safdari* [B], *Elham Amini*[B] *and Javier Palarea-Albaladejo* [C]

[A]USDA Forest Service, Pacific Southwest Research Station, Riverside, CA 92507, USA.
[B]Department of Chemical Engineering, Brigham Young University, Provo, UT 84602, USA.
[C]Biomathematics and Statistics Scotland, EH9 3FD Edinburgh, Scotland, UK.
[D]Corresponding author. Email: david.weise@usda.gov

**Abstract.** Pyrolysate gas mixtures are multivariate and relative in nature. Statistical techniques applied to these data generally ignore their relative nature. Published data for permanent gases (CO, $CO_2$, $H_2$, $CH_4$) and tars produced by pyrolysing 15 wildland fuels were reanalysed using compositional data analysis techniques. Mass and mole fractions were compositionally equivalent. Plant species, moisture status and heating mode effects on compositional balances formed from subsets of pyrolysates were tested. Plant species affected the amount of phenol, primary and secondary/tertiary tars relative to permanent gases and relative amounts of single- and multi-ring compounds. Plant moisture status affected the amount of CO relative to other permanent gases, of $H_2$ to $CH_4$ and tars to phenol. Heating mode and rate strongly influenced pyrolysate composition. Slow heating produced more primary tars relative to multi-ring tars than fast heating convective and combined radiant and convective heating modes. Slow heating produced relatively more compounds with fewer rings and fast heating produced relatively more multi-ring compounds. Compositional data analysis is a well-developed statistical methodology, providing models and methods equivalent to traditional ones, that accounts for the special constraining features of relative data. Future analysis of the compositional data related to wildland fire using compositional techniques is recommended.

**Keywords:** balance, CoDA, *Ilex*, log-ratio, *Morella*, palmetto, *Pinus palustris*, pyrolysis, *Quercus*, smoke, *Vaccinium*.

Received 6 August 2020, accepted 6 May 2021, published online 14 June 2021

## Introduction

Wildland fire is a complex phenomenon comprising chemical and physical processes. Two of the chemical processes that are key to wildland fire are pyrolysis and combustion (Shafizadeh 1984; Ward 2001) of plant material (a subset of biomass). During pyrolysis, a solid wildland fuel is heated and breaks down into constituent parts consisting of gases, tars and a solid material called char (Shafizadeh and Fu 1973; Shafizadeh 1982; Di Blasi 2008). During combustion, pyrolysis products react with oxygen, releasing energy and a large assortment of gaseous and solid chemical compounds (e.g. Andreae and Merlet 2001; Akagi *et al.* 2011; May *et al.* 2014). Data describing combustion products and air quality have been shown to be relative data known as compositional data (Jarauta-Bragulat *et al.* 2016; Weise *et al.* 2020*a*, 2020*b*; Gibergans-Baguena *et al.* 2020). Although the reactions comprising pyrolysis and combustion are complex and varied, a recent equation for the slow pyrolysis of lignocellulosic pecan (*Carya illinoinensis* (Wangenh.) K. Koch) shell waste can be used to illustrate some statistical properties associated with the composition of pyrolysis products (LeBlanc *et al.* 2016).

$$C_{33.42}H_{45.95}O_{20.26}N_{0.22}S_{0.14} = 0.50C_{20.08}H_{57.21}O_{22.46}N_{0.20}S_{0.22} + 1.72H_2O + 0.10H_2 + 1.07CH_4 + 0.02C_2H_4 + 0.06C_2H_6 + 2.21CO_2 + 2.05CO + 0.28C_{63.75}H_{32.47}O_{3.23}N_{0.43}S_{0.12} \quad (1)$$

The pyrolysis products on the right-hand side of Eqn 1 represent a near complete conversion (99.76%) of the lignocellulosic fuel, which seldom occurs in wildland fire. There are numerous products whose quantity is constrained due to the balanced equation. Focusing on the reactant (left-hand side), the composition of biomass consists of cellulose, hemicellulose, lignin, non-structural sugars, starches, lipids, proteins, pectin, phenol, silicates and minerals (e.g. Hough 1969; Shafizadeh 1982; Rogers *et al.* 1986; Collard and Blin 2014; Jolly *et al.* 2016; Matt *et al.* 2020). Molecular mass is conserved because these components break

**Table 1. Example illustrating how ordinary correlation of relative data such as terpene content (mg $g^{-1}$ dry weight) produces spurious results**

Data adapted from Romero *et al.* (2019). Shading indicates correlation coefficient with $P$ value <0.05

| α-pinene | β-pinene | Myrcene | Δ3-carene | Limonene | Sabinene hydrate | Terpinene | Caryophyllene |
|---|---|---|---|---|---|---|---|
| Original data | | | | | | | |
| 0.094 | 0.038 | 0.001 | 0.012 | 0.064 | 0.021 | 0.068 | 0.001 |
| 0.289 | 0.034 | 0.001 | 0.144 | 0.015 | 0.001 | 0.001 | 0.013 |
| 0.22 | 0.151 | 0.459 | 0.016 | 0.026 | 0.001 | 0.001 | 0.905 |
| 0.376 | 0.545 | 0.193 | 0.392 | 0.309 | 0.204 | 0.120 | 0.008 |
| 0.482 | 0.602 | 0.213 | 0.419 | 0.266 | 0.159 | 0.178 | 0.009 |
| 0.186 | 0.011 | 0.001 | 0.125 | 0.001 | 0.001 | 0.010 | 0.114 |
| Full composition after closure | | | | | | | |
| 0.314 | 0.127 | 0.003 | 0.040 | 0.214 | 0.070 | 0.227 | 0.003 |
| 0.580 | 0.068 | 0.002 | 0.289 | 0.030 | 0.002 | 0.002 | 0.026 |
| 0.124 | 0.085 | 0.258 | 0.009 | 0.015 | 0.001 | 0.001 | 0.509 |
| 0.175 | 0.254 | 0.090 | 0.183 | 0.144 | 0.095 | 0.056 | 0.004 |
| 0.207 | 0.259 | 0.092 | 0.180 | 0.114 | 0.068 | 0.077 | 0.004 |
| 0.414 | 0.025 | 0.002 | 0.278 | 0.002 | 0.002 | 0.022 | 0.254 |
| Subcomposition with no caryophyllene | | | | | | | |
| 0.315 | 0.128 | 0.003 | 0.040 | 0.215 | 0.070 | 0.228 | |
| 0.596 | 0.070 | 0.002 | 0.297 | 0.031 | 0.002 | 0.002 | |
| 0.252 | 0.173 | 0.525 | 0.018 | 0.030 | 0.001 | 0.001 | |
| 0.176 | 0.255 | 0.090 | 0.183 | 0.144 | 0.095 | 0.056 | |
| 0.208 | 0.260 | 0.092 | 0.181 | 0.115 | 0.069 | 0.077 | |
| 0.555 | 0.033 | 0.003 | 0.373 | 0.003 | 0.003 | 0.030 | |
| Pearson correlation coefficient ($r$) | | | | | | | |
| α-pinene | –0.58 | –0.77 | 0.70 | –0.28 | –0.46 | –0.12 | –0.31 |
| | –0.93 | –0.43 | 0.70 | –0.59 | –0.72 | –0.29 | |
| β-pinene | | 0.17 | –0.14 | 0.62 | 0.88 | 0.27 | –0.54 |
| | | 0.30 | –0.49 | 0.50 | 0.73 | 0.11 | |
| myrcene | | | –0.62 | –0.25 | –0.12 | –0.37 | 0.7 |
| | | | –0.61 | –0.29 | –0.30 | –0.39 | |
| Δ3-carene | | | | –0.4 | –0.21 | –0.46 | –0.38 |
| | | | | –0.55 | –0.32 | –0.45 | |
| Limonene | | | | | 0.88 | 0.89 | –0.67 |
| | | | | | 0.87 | 0.88 | |
| Sabinene hydrate | | | | | | 0.62 | –0.67 |
| | | | | | | 0.6 | |

down thermally by various temperature-dependent pathways (Shafizadeh 1982; Neves *et al.* 2011; Sekimoto *et al.* 2018). Because mass is conserved, an increase in the amount of one pyrolysis product species must result in a concomitant decrease in one or more of the other pyrolysis product species; hence the amounts on the right-hand side are intrinsically linked. After pyrolysis has occurred, the amounts of pyrolysis gas species relative to $O_2$ are key measures for successful ignition and flame spread, known as the lower and upper flammability limits.

Product species mass and mole fractions measured during pyrolysis of biomass are a prime example of compositional data. Being compositional data, the information contained in the data resides in the ratios between the product species (Aitchison 1986). Pyrolysis data have been expressed as relative measures such as concentrations, mixing ratios, mole fractions, mass fractions and volume fractions. The approach to statistical analysis of the composition of pyrolysis products has to date often ignored the intrinsic multivariate and relative nature of the data. Compositional data analysis (CoDA) is an approach that explicitly considers the statistical properties of multivariate relative data (Aitchison 1986).

Aitchison (2003) showed for illustration how two scientists examining the correlation between animal, vegetable, mineral and water proportions of a sample can arrive at very different conclusions if one scientist dried the sample, removing all water before calculating the correlations between the components. This is an example of subcompositional incoherence; that is, results differing depending on working with the full composition or a subset of it, which lead in part to Aitchison's seminal development of CoDA (Aitchison 1986). We present a similar example (Table 1) using terpene measurements previously reported (Romero *et al.* 2019). The original terpene content (mg $g^{-1}$ dry matter) comprises a composition of $D$ parts, which were put on a consistent relative scale by applying the closure operation,

$$C(\mathbf{x}) = \frac{[x_1, x_2, \ldots, x_D]}{\sum_{i=1}^{D} x_i} \quad (2)$$

which divides the amount for each gas ($x_i$) by the sum of amounts and expresses the data as fractions of a total, this total being 1 by default. $C(\mathbf{x})$ becomes a vector of proportions (mass fractions in this case), but in general it can be any other total by simple multiplication (e.g. $C(\mathbf{x}) \times 10^2$ for mass percentages or $C(\mathbf{x}) \times 10^6$ for parts per million by mass). Note that $C(\mathbf{x})$ is equivalent to the calculation used to determine mole fractions, mass fractions and mixing ratios (McNaught *et al.* 1997). After closure, the α-pinene content of 0.094 mg $g^{-1}$ dry matter became the proportion 0.314. Although the initial work on CoDA explicitly assumed in the definition of a composition that the parts sum (i.e. are closed) to a constant total, theory has developed to show that this is only a particular representation of the data in a simplex, and equivalent non-closed compositions carry the same relative information (Barceló-Vidal and Martín-Fernández 2016). On a related topic, the simplex has also been used as the basis for developing experimental designs for multispecies competition studies (Goelz 2001).

Regardless of the total, it is important to note that the resulting relativised data vector is equivalent to the original data and lives in what is known as a *D*-part simplex and, hence, statistical analysis of any equivalent representation of the data should provide the same results. In the example in Table 1, $D = 8$ for the full composition. The familiar Pearson correlation coefficient ($r$) was then calculated for all pairs of terpenes. In the full composition, α-pinene was not significantly negatively correlated with β-pinene, with an $r = -0.58$ ($P$ value $= 0.23$), while in the subcomposition missing caryophyllene, $r = -0.93$ ($P$ value $= 0.01$). Note that several correlation coefficients changed. If the correlation coefficient was statistically tested for equality to 0 using unadjusted $P$ values, the correlations that would be identified as significant at the usual statistical significance level of 0.05 are identified by shading. The pinenes were not negatively correlated in the full composition, but were negatively correlated in the subcomposition. Similarly, β-pinene was positively correlated with sabinene hydrate in the full composition, but not in the subcomposition. If the $P$ values were adjusted for false discovery rate using the method of Benjamini and Hochberg (1995), none of the correlations would be deemed different from 0.

The point of the illustration is that this index (Pearson correlation coefficient), which is generally trusted as a measure of pairwise association, can produce different results depending on something that should not affect it. This is an artefact unrelated to the actual relationship between the variables and, hence, the ordinary correlation coefficient is not a reliable measure with this type of data. Several statistical methods (e.g. linear regression) rely on correlations, so they are also affected by this problem. Instead, measuring associations in terms of proportionality is a coherent and meaningful alternative to ordinary correlation for compositional data (Egozcue *et al.* 2014, 2018; Lovell *et al.* 2015). Balance association (or b-association for short) has been developed as a statistical measure of proportionality (Egozcue *et al.* 2018). A measure of b-association, $\phi$, was defined and used to formulate the so-called unitary slope test relating one log-contrast of parts to another log-contrast (Lovell *et al.* 2015; Egozcue *et al.* 2018). An alternative approach describes the relationship between two parts in terms of the relationship of the dominance of each part relative to an average of all other parts in the composition (Kynčlová *et al.* 2017; Reimann *et al.* 2017; Filzmoser *et al.* 2018). A measure ranging in [–1,1], as does the familiar Pearson correlation coefficient ($r$), is obtained.

A well principled statistical methodological body for CoDA has been developed in the past 30 years and this is an active area of statistical research (Aitchison 1986; Barceló-Vidal *et al.* 2001; Lovell *et al.* 2015; Pawlowsky-Glahn *et al.* 2015; Filzmoser *et al.* 2018). Interestingly, this methodology has been successfully applied in varied fields, but appears to have seldom been applied to combustion or emissions data from wildland fire (Bandeen-Roche 1994; Billheimer 2001; Buccianti and Pawlowsky-Glahn 2006; Jarauta-Bragulat *et al.* 2016; Speranza *et al.* 2018; Gibergans-Baguena *et al.* 2020; Weise *et al.* 2020*b*).

In order to use familiar statistical techniques, the mainstream approach in CoDA currently is to transform the parts from the simplex where they reside to coordinates in the usual real space using isometric log-ratio (*ilr*) coordinates (Egozcue and Pawlowsky-Glahn 2005). Software to perform CoDA is available, including the stand-alone point-and-click *CoDaPack* package (Thió-Henestrosa and Comas 2016) (http://www.compositionaldata.com/codapack.php) and comprehensive libraries on the open-source R statistical computing system (R Core Team 2020): *compositions* (van den Boogaart and Tolosana-Delgado 2013), *robCompositions* (Templ *et al.* 2011) and *zCompositions* (Palarea-Albaladejo *et al.* 2014; Palarea-Albaladejo and Martín-Fernández 2015).

With the above considerations borne in mind, the objective of this study was to reanalyse compositional data from pyrolysis of several plant species native to the southern United States (Safdari *et al.* 2018, 2019, 2020; Amini *et al.* 2019) to determine if the composition of pyrolysis products was affected by (a) plant species, (b) whether the samples were fresh or air-dried and (c) the heating method (convective and/or radiant, slow vs fast), using analysis of variance within a CoDA framework. We hope to demonstrate that the CoDA approach can shed as much or more light on the relationships in and between the pyrolysis data by applying techniques consistent with the multivariate and relative nature of the data instead of using ordinary methods that have ignored this fact as performed previously (Safdari *et al.* 2018, 2019, 2020; Amini *et al.* 2019). As part of the larger study, the yield (mass) of pyrolysis products was also measured but is not analysed here. Aitchison and Egozcue (2005) discussed the relative nature of compositional data and the limitations on inferences that can be made based solely on compositions. Inclusion of external information such as mass, environmental variables etc. can be used to strengthen inferences based solely on the relative information contained in compositions. This analysis will focus only on the product species composition of pyrolysis products.

## Statistical methods

As part of a larger study to measure and model pyrolysis of wildland fuels to advance our ability to use physically-based models of wildland fire behaviour (Weise *et al.* 2018), the composition of gases released by pyrolysis of wildland fuels has been measured at the bench scale (Safdari *et al.* 2018, 2019, 2020; Amini *et al.* 2019), in fuel beds burned in a wind tunnel (Phillips *et al.* 2020; Aminfar *et al.* 2020) and in small, prescribed burns in

the field (Scharko *et al.* 2019*a*, 2019*b*). As experiments increased in size from bench to field, the number of parts measured (number of gases) decreased due to instrument limitations and the number of plant species considered also decreased due to increased cost of larger laboratory and field experiments. A meaningful comparison of the plant species data from these multi-scale experiments therefore requires a more sophisticated compositional data analysis.

### *Data description and preprocessing*

The bench-scale experiments conducted at Brigham Young University (BYU) measured the product species composition of pyrolysis on a dry basis from nursery-cultivated plants from 14 different species (Table 2) as a function of plant moisture status (fresh or dried) and heating mode (convective and radiative) (Safdari *et al.* 2018, 2019, 2020; Amini *et al.* 2019). (Scientific names will be used in tables and figures.) Ultimate, proximate and summative analyses of the plant samples have been reported (Safdari *et al.* 2018; Matt *et al.* 2020). The BYU gas data consisted of four permanent gases (PGs: $H_2$, CO, $CO_2$, $CH_4$) and the tars, which can then form secondary pyrolysis products. Plant foliage samples were heated by three different modes with a radiant panel and/or post-flame fuel-rich gases in a flat-flame burner (FFB) (Safdari *et al.* 2018, 2020), providing a fuel-rich environment that was $O_2$-free. These experiments were similar to other pyrolysis experiments with one notable exception—the foliage samples retained both moisture and their physical shape (as opposed to the traditional ground samples (e.g. Susott 1982)).

The three FFB heat fluxes were nominally 50, 100 and 150 kW $m^{-2}$ and heating rates were 4, 180 and 195°C $s^{-1}$ for radiant only, convective only and radiant + convective modes, respectively. A total of 64 compounds (4 PGs and 60 tars) were identified in the FFB experiments. The composition of the fuel-rich gas mixture ($CO_2$, $H_2O$, CO) used for heating was subtracted from the collected pyrolysis gas samples to provide the composition of the pyrolysis gases. Slow pyrolysis (heating rate of 0.5°C $s^{-1}$) performed in an electrically-heated pyrolyser in an $N_2$ ($O_2$-free) environment (Amini *et al.* 2019) comprised the fourth heating mode investigated. The nominal gas temperatures for the four heating modes were 500°C, 105°C, 765°C and 804°C for the pyrolyser, radiant, convective and radiant + convective modes, respectively. The four heating modes were designated as Slow, Rad, Conv and RadConv for the pyrolyser and three FFB modes, respectively. In the pyrolyser experiment, 299 compounds (4 PGs and 295 tar compounds) were identified using the same analytical methods. A subset of 37 compounds was common to both apparatuses. In total, 326 organic compounds were identified in the FFB and pyrolyser. The effect of heating rate on the product composition (light gas, tar, char) and on the individual parts was previously evaluated by interpreting bar charts and the standard error of each proportion (Amini *et al.* 2019; Safdari *et al.* 2019).

Heating rates of 75–5000°C $s^{-1}$ have been reported for air near foliar fuels in the canopy of shrubs and trees, which are more akin to fast pyrolysis and conditions in the FFB (Butler *et al.* 2004, 2016; Tachajapong *et al.* 2008). The slow pyrolysis instrument was used to be comparable with earlier work in wildland fuels (e.g. Susott 1982). Prior pyrolysis work has described the need to conduct experimental work under well-controlled conditions due to the complexity of thermal behaviour chemically and physically as opposed to conducting this work during actual fires under field conditions with limited control of conditions (Dimitrakopoulos 2001*b*). To bridge the gap between well-controlled pyrolysis experiments and actual wildland fire conditions, different approaches have been used. Ignition behaviour has been correlated with thermal characteristics of wildland fuels (Dimitrakopoulos 2001*a*; Liodakis *et al.* 2002; Zhang *et al.* 2011). Fire hazard maps based on caloric values and flammability correlated with chemical and physical properties of the fuels have been produced (e.g. Núñez-Regueira *et al.* 1999; Ryan and Opperman 2013). These fire hazard maps capture only a subset of the factors that contribute to risk (Hardy 2005). Although these approaches can produce useful information that can be used to manage wildland fire risks, they are based, in part, on the assumption that the bench-scale results for pyrolysis apply at larger scales. The primary objective of the larger project was to test that assumption. We categorised the FFB and pyrolyser experiments as well-controlled pyrolysis experiments because the heating rates and temperatures were tightly controlled and gas sampling occurred in an inert or $O_2$-free (fuel-rich) environment.

In the FFB and pyrolyser experiments, three replications of 14 plant species in two moisture conditions (freshly picked or air-dried for several days) heated convectively and radiantly, singly and in combination were performed. Air-dried fuels consisted of samples cut from the living plants and allowed to dry out for 1 week in a laboratory under ambient building conditions (temperature 23–26°C, atmospheric pressure 850–865 mbar and relative humidity of 10–20%). The moisture content of the air-dried fuels was typically less than 10% on a dry mass basis (Amini *et al.* 2019). A 15th fuel, litter (i.e. dry, dehisced and aged foliage of longleaf pine) was included as it is a major component of the understory fuel complex (Table 2). This inclusion enabled comparison of three types of longleaf pine

**Table 2. Common plant species of pine forests of the southern USA used in Brigham Young University pyrolysis experiments**

| Species[A] | Common name | Growth form |
|---|---|---|
| *Aristida stricta* Michx. | Wiregrass | Grass |
| *Schizachyrium scoparium* (Michx.) Nash | Little bluestem | Grass |
| *Ilex glabra* (L.) A. Gray | Inkberry | Evergreen shrub |
| *Ilex vomitoria* Aiton 'Schelling Dwarf' | Yaupon | Deciduous shrub |
| *Lyonia lucida* (Lam.) K. Koch | Fetterbush | Deciduous shrub |
| *Morella cerifera* (L.) Small | Wax myrtle | Evergreen shrub |
| *Persea palustris* (Raf.) Sarg. | Swamp bay | Evergreen shrub |
| *Vaccinium arboreum* Marshall | Sparkleberry | Deciduous shrub |
| *Vaccinium darrowii* Camp 'Rosa's Blush' | Darrow's blueberry | Deciduous shrub |
| *Quercus nigra* L. | Water oak | Deciduous tree |
| *Quercus virginiana* Mill. | Live oak | Evergreen tree |
| *Sabal minor* (Jacq.) Pers. | Dwarf palmetto | Palm |
| *Serenoa repens* (W. Bartram) Small | Saw palmetto | Palm |
| *Pinus palustris* Mill. (needles) | Longleaf pine foliage | Evergreen conifer |
| *Pinus palustris* Mill. (litter) | Longleaf pine litter | Cast foliage |

[A]USDA (2020).

foliage, which resulted in the original dataset containing 348 observations. Fuel beds burned in the wind tunnel and field burns of the larger study (Scharko *et al.* 2019*a*; Banach *et al.* 2021) were composed of a subset of the individual plant species and longleaf pine litter. Describing the pyrolysis gas composition of the pine needles was necessary to study linkages between the bench, wind tunnel and field-scale measurements.

The moisture status effect is a general term meant to account for the two (or three for longleaf pine) different foliage conditions. Any differences between the foliage conditions cannot be tied to a specific cause such as lower moisture content, cell wall or nucleus changes or conversion of cellular contents by plant physiological processes or decay. The gas collection process removed water from the sample before the composition was determined; however, the CoDA approach guarantees that this removal does not affect the relationships between the relative amounts of the other components (Aitchison 1986).

Mean values for the radiation-only heating mode were used in the present analysis because the original data for the tar analysis were unavailable. The total dataset used in the present analysis therefore included 290 observations. Information on the molecular mass and chemical classification was extracted from the PubChem database (Kim *et al.* 2019). All statistical analyses were performed using version 3.6.3 of the R statistical system (R Core Team 2020).

The four permanent gases and 322 organic compounds contained in the tar comprised a dataset in which each sample contained 326 parts (compounds). In the original data, mole fraction was calculated separately for the light gases and tars. In the full dataset, 89.19% of the values were below detection limits (BDL). Nearly 190 of the identified compounds were detected in only single combinations of plant species by heating mode. After removing the compounds that were measured in less than 4 of 60 heating mode/species combinations, $D = 88$ compounds remained with a BDL rate of 64.05%. Thus, in the current analysis, each sample consisted of a vector $\mathbf{x} = [x_1 \ldots x_{88}]$ where parts $x_1 \ldots x_{88}$ were the measured mole fractions. An average of 52 compounds were measured in the pyrolyser and averages of 34, 37 and 30 compounds were recorded for the FFB radiation, convection and radiation + convection modes, respectively. The multiplicative Kaplan–Meier smoothing spline algorithm included in the *zCompositions* package was used to impute the values BDL in the mole fraction data, with a uniform small value (1E-06) set as the detection limit while multiplicatively adjusting the entire composition to account for the relative scale of the data (Palarea-Albaladejo and Martín-Fernández 2015). Note that in the CoDA context, the conversion from mole fraction composition $x$ into mass fraction composition $y$ corresponds to the basic perturbation operation ($\oplus$; Aitchison (1986); equivalent in the simplex to addition in the ordinary real space), $\mathbf{y} = \mathbf{x} \oplus \mathbf{p} = C[x_1 p_1, \ldots, x_d p_d]$, where $\mathbf{p} = [p_1, \ldots, p_D]$ is a perturbation vector. As stressed above, statistical results should be equivalent regardless of the units of the composition and this is guaranteed by the log-ratio approach to CoDA, fulfilling the so-called scale and perturbation invariance principles (van den Boogaart and Tolosana-Delgado 2013).

In the following sections, we introduce some basic compositional analyses conducted using pyrolysis data. These analyses can also be applied to other compositional data associated with wildland fire such as smoke emissions (Weise *et al.* 2020*a*; 2020*b*), plant and animal species occurrence/productivity, fuel loading/distribution, fire cost distribution and distribution of energy release by heat transfer mode, to name a few.

### *Compositional summary statistics*

The original data were expressed as mole and mass fractions and were closed because they were expressed as proportions of the total number of moles or total mass (Eqn 2). However, the PGs and tars were closed separately and were subcompositions of the full composition of measured pyrolysis products. In the present study, the mole fractions for the PGs and tars were combined into a single observation for each sample and then closed. Note that these operations preserve the original relative information conveyed by the data and, hence, do not affect the results from compositional analysis. Compositional summary statistics consisting of the centre, the total variance and the variation array were estimated (Aitchison 1986). The centre ($\bar{\mathbf{g}}$) is the closed vector of geometric means for each part estimated as

$$\hat{\mathbf{g}} = C[\hat{g}_1, \hat{g}_2, \ldots, \hat{g}_D] \tag{3}$$

where $\hat{g}_j = \left(\prod_{i=1}^{n} x_{ij}\right)^{1/n}, j = 1, 2, \ldots, D$. Although there are different measures for the variability of compositional data (van den Boogaart and Tolosana-Delgado 2013), a common summary is given by the variances of the log-ratios of parts $i$ and $j$ $(\tau_{ij})$; thus the variation matrix $\mathbf{V}$ is a $D \times D$ symmetric matrix containing elements estimated from the data by

$$\hat{\tau}_{ij} = \mathrm{var}\left(\ln \frac{x_i}{x_j}\right) \tag{4}$$

where $i$ and $j$ range from 1 to $D$ and var is the usual sample variance. The total (metric) variance (*mvar*) can be obtained from $\hat{\tau}_{ij}$ as

$$\mathrm{mvar}(\mathbf{x}) = \frac{1}{D} \sum_{i<j} \hat{\tau}_{ij} \tag{5}$$

(Pawlowsky-Glahn and Egozcue 2001). In general, the smaller the values of $\hat{\tau}_{ij}$, the more proportional are the parts involved. The compositional centre and the metric variance were calculated for the mole fraction representation of the data. Estimating proportionality between all possible pairs of parts by either method (Kynčlová *et al.* 2017; Egozcue *et al.* 2018) would result in 3828 pairwise comparisons, which is difficult to interpret so it was not calculated.

### *Log-ratio balances and multivariate analysis of variance*

Aitchison (1986) originally proposed expressing compositional data as log-ratios. In particular, the additive log-ratio (*alr*) transformation, which uses an arbitrary part of the composition (part $D$) as a common denominator, was generally suggested in order to apply statistical inference methods. Although useful in parametric statistical modelling, the *alr* is particularly inadequate when distances, angles or shapes are involved (e.g. when performing clustering analysis or multidimensional scaling) as it

deforms these (Aitchison 1986; Aitchison *et al.* 2000; van den Boogaart and Tolosana-Delgado 2013). Alternatively, the isometric log-ratio (*ilr*) transforms compositional data into real-valued coordinates, which preserves distances and enables the use of a wider range of statistical methods to analyse the data (Egozcue *et al.* 2003). An inconvenience of the *ilr* approach is that the practical interpretation of generic *ilr* coordinates can be challenging. In fact, an infinite number of *ilr* coordinate systems can be formed from the same composition by orthogonal rotations. Hence, any statistical method to be used should be checked for invariance to these rotations. This is the case for many common techniques. Moreover, the ability to define alternative *ilr* coordinate systems allows the practitioner to tailor them to be meaningful for the research question of interest.

The conventional approach to smoke emissions calculations for regulatory purposes is to determine the amount of gases produced that exceeds normal atmospheric levels. Although atmospheric levels of gases have fluctuated dramatically over the history of the planet (e.g. Ehleringer and Cerling 1995), atmospheric pollutants are quantified relative to the current composition of the atmosphere, which on a volumetric basis (in percentages) is 78.08 $N_2$, 20.95 $O_2$, 0.934 Ar, 0.04 $CO_2$, 0.0018 Ne, 0.00052 He, 0.00017 $CH_4$, 0.00011 Kr and 0.000055 $H_2$ (Williams 2020). All other gases comprise the small remaining fraction. The excess mixing ratio is $\Delta gas_j = \{gas_j\}_{sample} - \{gas_j\}_{background}$ where *background* denotes the ambient amount of the gas (Ward and Radke 1993; Urbanski *et al.* 2008). Generally, the ambient amounts of biomass gases other than $CO_2$ and $CH_4$ are near or at zero. Expressing emission data as ratios between a gas of interest and either CO or $CO_2$ is a common method (e.g. Crutzen *et al.* 1979; Andreae *et al.* 1988). Thus, emission ratios can be defined as $ER_{CO}(gas_j) = \frac{\Delta gas_j}{\Delta CO}$. Applying this to the entire composition $x$ of smoke we have that $ER_{CO}(\mathbf{x}) = \left[\frac{\Delta gas_1}{\Delta CO}, \ldots, \frac{\Delta gas_j}{\Delta CO}\right]$. Note that taking the logarithm of $ER_{CO}(\mathbf{x})$ is in fact equivalent to applying the *alr* transformation to $x$ where ΔCO is the reference part $x_D$.

$$alr(\mathbf{x}) = \left[\ln\frac{x_1}{x_D}, \ldots, \ln\frac{x_k}{x_D}\right] = \left[\ln\frac{\Delta gas_1}{\Delta CO}, \ldots, \ln\frac{\Delta gas_k}{\Delta CO}\right] = \ln(ER_{CO}(\mathbf{x})), k = 1, \ldots, D-1 \quad (6)$$

The pyrolysis gases in the present analysis were differenced with the ambient atmosphere within each instrument. For the pyrolyser and the FFB in Rad mode, the ambient atmosphere was $N_2$, which did not require subtraction; the ambient atmosphere in the FFB for Conv and RadConv modes contained post-flame combustion gases, which were subtracted. The point of including Δ in Eqn 6 is to show that the present log-ratio approach is different from other prior analyses involving emission ratios. Prior analyses could be easily redone simply by applying appropriate log-ratio transformations (Weise *et al.* 2020*a*).

We were interested in the effects of the experimental factors (plant species, heating mode and moisture status) on the relative dominance between groups of gases. We first used generic *ilr* coordinates in a three-way multivariate analysis of variance (MANOVA) model (van den Boogaart and Tolosana-Delgado 2013). Note that the MANOVA overall effect tests provide identical results using either *alr* or any *ilr* coordinate system. When the interaction terms were statistically significant, interaction plots were used to understand the nature of the interaction and determine if the interaction terms could be removed. Interpretability was enhanced by transforming the fitted values back into compositions by *ilr* inverse transformation and plotting the log-ratio of the centre obtained for each experimental factor category to the overall centre in an ordinary barplot format

$$\left(average\ deviation_{log-scale}\right)_i = \log\left(\frac{\hat{g}_{factor_j}\big)_{\boldsymbol{i}}}{\hat{g}_i}\right), \quad \boldsymbol{i} = 1, \ldots, D; j = 1, \ldots, m \quad (7)$$

where $m$ is the number of levels of effect $j$ providing further insight into trends in the effects (Montero-Serrano *et al.* 2010; Butler *et al.* 2020). For the present experiment, $m$ was 15, 4 and 2 for plant species, heating mode and moisture status, respectively.

To examine the significance of interaction terms in the MANOVA, marginal means were calculated using procedures from the *emmeans* package (Lenth 2020). Marginal means for each particular combination of plant species, heating mode and moisture status were calculated from each observation, which consisted of 87 balances (*ilr* coordinates) in which the gases appeared in either the numerator, denominator or not at all depending on the ratio. For a multivariate linear model, the *emmeans* procedure creates a factor variable distinguishing the multivariate responses (the *ilr* coordinates) across which the marginal means are estimated.

Meaningful statistical analysis of compositions is conducted on log-ratios between their parts. We were interested in defining these log-ratios so that we were able to determine the effects of plant species, heating mode and moisture status on groups of compounds potentially related to combustion and smoke production. Egozcue and Pawlowsky-Glahn (2005) devised a sequential binary partitioning procedure to define tailored *ilr* coordinates representing comparisons between scientifically meaningful subsets of parts of a composition. This family of *ilr* coordinates, known as compositional balances $\tilde{z}_k$, is defined as

$$\tilde{z}_k = \sqrt{\frac{r_k s_k}{r_k + s_k}} \ln\left[\frac{\left(\prod_{i=1}^{r_k} x_{k_i}^{+}\right)^{1/r_k}}{\left(\prod_{j=1}^{s_k} x_{k_j}^{-}\right)^{1/s_k}}\right], \quad k = 1, \ldots, D-1 \quad (8)$$

where the log-ratio term compares the geometric mean of $r_k$ parts in one subset (in the numerator, indicated with + symbol) with the geometric mean of $s_k$ parts in another subset (in the denominator, indicated with – symbol). The preceding multiplicative factor is a normalisation factor formally required to ensure comparability of the balances. A simpler expression as the normalised difference between the means of log-transformed data is given by

$$\tilde{z}_k = \sqrt{\frac{r_k s_k}{r_k + s_k}}\left(\frac{1}{r_k}\sum_{i=1}^{r_k} \ln x_{k_i}^{+} - \frac{1}{s_k}\sum_{j=1}^{s_k} \ln x_{k_j}^{-}\right), \quad k = 1, \ldots, D-1 \quad (9)$$

Pyrolysates were categorised as PGs and tars. Safdari *et al.* (2020) further categorised tar compounds into five groups (phenol, phenol derivatives, 2-ring aromatics, 3–5-ring aromatics and other hydrocarbons) and examined the effect of heating mode on these groups. We adapted the groups by splitting the 3–5-ring group into three groups (3-ring, 4-ring, 5-ring). Although Amini *et al.* (2019) classified the pyrolyser products as aromatic, oxidised aromatic, non-aromatic and containing nitrogen, we separated the pyrolysis products as above and further separated the other hydrocarbons into acids, alcohols, aldehydes, ketones and benzenoids. The sequential binary partition based on this categorisation resulted in 87 balances; of which 13 balances provided meaningful comparisons between the PG group ($H_2$, CO, $CO_2$, $CH_4$) and the 11 tar groups (Table 3). Each balance compared the relative dominance of the two groups of parts involved. The remaining 74 balances are not presented here; however, they were necessary to determine the full representation of the composition to conduct the multivariate tests.

A set of balance *ilr* coordinates was thus created using the above procedure. Note that because of scale and perturbation invariance, as well as the properties of the *ilr* transformation, the MANOVA results for the mole and mass fraction data are identical except for the value of the intercept term (which simply represents the change of units as a translation). Pairwise comparisons of the effects of plant species, heating mode and moisture status on the defined balances were made using univariate *t*-tests with *P* values adjusted to control the false discovery rate (Benjamini and Hochberg 1995). Again, the effect estimates used in the pairwise comparisons did not differ between mole and mass fraction form. Because the *ilr* coordinates are real-valued (as opposed to being defined on the simplex as the original composition), the overall mean value for each balance could be subtracted as ordinarily done from the balance mean value for each experimental factor category and then plotted in an ordinary barplot format to identify trends (Montero-Serrano *et al.* 2010). A value less than zero for the average effect suggested that the experimental factor category reduced the relative amount of pyrolysis gases in the balance numerator compared with the overall mean ratio.

## Results and discussion

### *Compositional summary statistics*

Proximate analysis showed that the plant species were similar in terms of ash content, volatile matter and fixed carbon; ultimate analysis showed C, H, N, S, and O composition within accepted ranges (Safdari *et al.* 2018). Summative analysis provided a description of lipids, non-structural sugars, protein, pectin, starch, phenol, silicates, minerals, cellulose, hemicellulose and structural lignin (Matt *et al.* 2020). The summative analysis identified differences in composition of the leaf samples based on error measures; however, these differences have not been analysed using CoDA methods as yet. Future work will compare plant composition with pyrolysis composition in a CoDA framework.

The range in molecular weight of the products produced by the FFB (2–252.3 g $mol^{-1}$) was much smaller than the range observed in the pyrolyser (2–593 g $mol^{-1}$). The unweighted arithmetic mean molecular weights in the FFB and pyrolyser were 138.3 and 162.3 g $mol^{-1}$, respectively. The compositional centre (mean) showed the relative dominance of CO (Table 4) in the pyrolysis products on a mole fraction basis and the relative dominance of phenol on a mass fraction basis. The PGs accounted for 81.4% of the composition on a mole fraction basis and 51.2% on a mass fraction basis. Phenol (12.4%) and three phenol derivatives (1,2-benzenediol, 4-methyl-phenol, 2,6-dimethoxy-phenol; 5.8%) accounted for an additional

**Table 3. Schematic illustrating the construction of balances of groups of compositional parts of scientific interest determined by sequential binary partition**

'+' denotes parts in numerator and ' – ' denotes parts in denominator of balance (an additional 74 balances not shown completed the full partition)

| | | Compositional part or group | | | | | | | | | | | | | | |
|---|---|---|---|---|---|---|---|---|---|---|---|---|---|---|---|---|
| | | CO | $H_2$ | $CO_2$ | $CH_4$ | Phenol | Phenol derivatives | Acid | Alcohol | Aldehyde | Ketone | Benzene | 2-ring | 3-ring | 4-ring | 5-ring |
| Balance | Tars vs PG[A] | – | – | – | – | + | + | + | + | + | + | + | + | + | + | + |
| | CO vs other PG | + | – | – | – | | | | | | | | | | | |
| | $H_2$ vs $CH_4$ | | + | | – | | | | | | | | | | | |
| | Tars vs phenol | | | | | – | + | + | + | + | + | + | + | + | + | + |
| | Primary vs other tars | | | | | | – | + | + | + | + | – | – | – | – | – |
| | Other tars vs phenol derivatives | | | | | | – | | | | | + | + | + | + | + |
| | Acid, alcohol vs other hydrocarbons (HC) | | | | | | | + | + | – | – | | | | | |
| | Aldehyde vs ketone | | | | | | | | | + | – | | | | | |
| | Acid vs alcohol | | | | | | | + | – | | | | | | | |
| | Benzene vs rings | | | | | | | | | | | + | – | – | – | – |
| | 2- and 3- vs 4- and 5-ring | | | | | | | | | | | | + | + | – | – |
| | 2- vs 3-ring tars | | | | | | | | | | | | + | – | | |
| | 4- vs 5-ring tars | | | | | | | | | | | | | | + | – |

[A]PG denotes permanent gases ($CH_4$, CO, $CO_2$, $H_2$).

**Table 4. Compositional summary statistics of permanent gases and tars comprising pyrolysis products of 14 species of southern USA wildland plants measured in a flat-flame burner and a pyrolyser**

Original data were mole fraction of permanent gases and mole fraction of tars

| Pyrolyzate | Amount[A] | Var[B] | $P^C$ | Mass[D] | Pyrolyzate | Amount | Var | $P$ | Mass |
|---|---|---|---|---|---|---|---|---|---|
| Carbon monoxide | 4.09E-01 | 0.03 | 2.30E-03 | 2.94E-01 | Phenol, 3,4-dimethyl- | 4.23E-07 | 1.62 | 1.00E-02 | 1.33E-06 |
| Hydrogen | 1.50E-01 | 0.03 | 1.66E-04 | 7.76E-03 | 1,2-Cyclopentanedione, 3-methyl- | 2.69E-07 | 1.47 | 9.22E-03 | 7.73E-07 |
| Carbon dioxide | 1.47E-01 | 0.03 | 3.62E-03 | 1.66E-01 | 2-Furancarboxaldehyde, 5-methyl- | 2.45E-07 | 1.49 | 9.05E-03 | 6.92E-07 |
| Phenol | 1.24E-01 | 0.05 | 7.74E-03 | 3.00E-01 | 2-Methoxy-4-vinylphenol | 1.78E-07 | 1.56 | 1.23E-02 | 6.87E-07 |
| Methane | 1.08E-01 | 0.03 | 1.32E-03 | 4.43E-02 | 1,3-Benzenediol, 4-ethyl- | 1.65E-07 | 1.31 | 1.14E-02 | 5.84E-07 |
| 1,2-Benzenediol | 2.39E-02 | 0.36 | 9.05E-03 | 6.74E-02 | 2-Cyclopenten-1-one | 1.14E-07 | 1.18 | 6.75E-03 | 2.40E-07 |
| Phenol, 4-methyl- | 2.36E-02 | 0.12 | 8.89E-03 | 6.55E-02 | 2-Methoxy-6-methylphenol | 1.01E-07 | 1.14 | 1.14E-02 | 3.59E-07 |
| Phenol, 2,6-dimethoxy- | 1.08E-02 | 0.51 | 1.27E-02 | 4.28E-02 | 2-Cyclopenten-1-one, 2-hydroxy- | 7.74E-08 | 1.13 | 8.07E-03 | 1.95E-07 |
| 1,4-Benzenediol | 2.00E-03 | 0.93 | 9.05E-03 | 5.64E-03 | 1-Octen-3-ol | 7.69E-08 | 0.92 | 1.05E-02 | 2.53E-07 |
| 1-Methylnaphthalene | 1.84E-04 | 1.50 | 1.17E-02 | 6.70E-04 | Maltol (Larixic acid) | 7.16E-08 | 1.04 | 1.04E-02 | 2.32E-07 |
| Naphthalene | 1.63E-04 | 1.47 | 1.05E-02 | 5.35E-04 | 2(3H)-Furanone | 7.08E-08 | 0.98 | 6.91E-03 | 1.53E-07 |
| Pyrene | 1.13E-04 | 2.21 | 1.66E-02 | 5.87E-04 | Phenol, 2-methoxy-4-(1-propenyl)- | 6.25E-08 | 0.99 | 1.35E-02 | 2.63E-07 |
| Fluoranthene | 8.48E-05 | 2.07 | 1.66E-02 | 4.40E-04 | 2(5H)-Furanone | 5.69E-08 | 1.03 | 6.91E-03 | 1.23E-07 |
| 1,2-Benzenediol, 4-methyl- | 8.47E-05 | 1.96 | 1.02E-02 | 2.70E-04 | 2-Pentanone, 4-hydroxy-4-methyl- | 5.68E-08 | 0.95 | 9.55E-03 | 1.69E-07 |
| Fluorene | 7.85E-05 | 2.06 | 1.37E-02 | 3.35E-04 | Ethanone, 1-(2-furanyl)- | 4.52E-08 | 0.85 | 9.05E-03 | 1.28E-07 |
| 7H-Benzo[c]fluorene | 7.60E-05 | 2.04 | 1.78E-02 | 4.21E-04 | 3-Furaldehyde | 4.29E-08 | 0.96 | 7.90E-03 | 1.06E-07 |
| Phenanthrene | 7.50E-05 | 2.02 | 1.47E-02 | 3.43E-04 | 2-Cyclopenten-1-one, 2-hydroxy-3-methyl- | 4.25E-08 | 0.86 | 9.22E-03 | 1.22E-07 |
| Phenol, 2-methyl- | 6.74E-05 | 1.70 | 8.89E-03 | 1.87E-04 | Phenol, 2-methoxy-4-methyl- | 4.23E-08 | 0.87 | 1.14E-02 | 1.50E-07 |
| Anthracene | 6.18E-05 | 1.93 | 1.47E-02 | 2.82E-04 | 1,2,3-Benzenetriol, 5-methyl- | 4.09E-08 | 0.59 | 1.15E-02 | 1.47E-07 |
| Benzo[e]pyrene | 5.66E-05 | 1.89 | 2.07E-02 | 3.66E-04 | 1,2-Cyclopentanedione | 4.00E-08 | 0.77 | 8.07E-03 | 1.01E-07 |
| 11H-Benzo[a]fluorene | 5.62E-05 | 1.89 | 1.78E-02 | 3.12E-04 | Benzyl alcohol | 3.54E-08 | 0.55 | 8.89E-03 | 9.83E-08 |
| Acenaphthylene | 5.59E-05 | 1.89 | 1.25E-02 | 2.18E-04 | 2-Cyclopenten-1-one, 2-methyl- | 3.39E-08 | 0.69 | 7.90E-03 | 8.35E-08 |
| Naphthalene, 2-phenyl- | 5.45E-05 | 1.89 | 1.68E-02 | 2.85E-04 | Benzoic acid | 3.34E-08 | 0.72 | 1.00E-02 | 1.05E-07 |
| Benzo[c]phenanthrene | 5.11E-05 | 1.85 | 1.88E-02 | 2.99E-04 | Benzoic acid, 4-hydroxy-, methyl ester | 3.04E-08 | 0.76 | 1.25E-02 | 1.19E-07 |
| Benzo(a)fluoranthene | 4.00E-05 | 1.75 | 2.07E-02 | 2.59E-04 | Propanoic acid, 2-propenyl ester | 2.65E-08 | 0.65 | 9.39E-03 | 7.76E-08 |
| Cyclopenta[cd]pyrene | 3.67E-05 | 1.72 | 1.86E-02 | 2.13E-04 | 4-Ethylcatechol | 2.61E-08 | 0.65 | 1.14E-02 | 9.24E-08 |
| Benz(a)anthracene | 3.63E-05 | 1.71 | 1.88E-02 | 2.13E-04 | Phenol, 3-methyl- | 2.33E-08 | 0.71 | 8.89E-03 | 6.47E-08 |
| Naphthacene | 3.56E-05 | 1.70 | 1.88E-02 | 2.08E-04 | Phenol, 2,5-dimethyl- | 2.33E-08 | 0.61 | 1.00E-02 | 7.30E-08 |
| Phenol, 2-methoxy- (guaiacol) | 3.40E-05 | 2.11 | 1.02E-02 | 1.08E-04 | Propanoic acid | 2.33E-08 | 0.58 | 6.09E-03 | 7.30E-08 |
| 2-Methylnaphthalene | 3.19E-05 | 1.99 | 1.17E-02 | 1.16E-04 | Ethanone, 1-(2-hydroxy-5-methylphenyl)- | 2.20E-08 | 0.55 | 1.23E-02 | 6.21E-08 |
| Chrysene | 2.48E-05 | 1.57 | 1.88E-02 | 1.45E-04 | Phenol, 3,4-dimethoxy- | 2.05E-08 | 0.56 | 1.27E-02 | 8.10E-08 |
| 1,2-Benzenediol, 3-methyl- | 8.40E-06 | 1.88 | 1.02E-02 | 2.68E-05 | Phenol, 2,6-dimethoxy-4-(2-propenyl)- | 2.03E-08 | 0.60 | 1.60E-02 | 1.01E-07 |
| Phenol, 4-ethyl- | 3.68E-06 | 2.12 | 1.00E-02 | 1.15E-05 | Naphthalene, 1,6,7-trimethyl- | 2.01E-08 | 0.57 | 1.40E-02 | 8.76E-08 |
| Indole | 3.65E-06 | 1.80 | 9.63E-03 | 1.09E-05 | 1,3-Benzenediol | 1.98E-08 | 0.51 | 9.05E-03 | 5.58E-08 |
| 1,2-Benzenediol, 3-methoxy- | 3.14E-06 | 1.89 | 1.15E-02 | 1.13E-05 | 2H-1-Benzopyran-2-one, 3,4-dihydro-6-hydroxy- | 1.96E-08 | 0.49 | 1.35E-02 | 8.26E-08 |
| 1,2,3-Benzenetriol | 2.33E-06 | 1.57 | 1.04E-02 | 7.53E-06 | Benzeneethanol, 4-hydroxy- | 1.96E-08 | 0.43 | 1.14E-02 | 6.93E-08 |
| Phenol, 4-ethyl-2-methoxy- | 1.82E-06 | 1.95 | 1.25E-02 | 7.11E-06 | Benzene, 1,4-diethyl- | 1.94E-08 | 0.44 | 1.10E-02 | 6.69E-08 |
| Benzofuran, 2,3-dihydro- | 1.25E-06 | 1.89 | 9.88E-03 | 3.86E-06 | 3,7,11,15-Tetramethyl-2-hexadecen-1-ol | 1.77E-08 | 0.49 | 2.44E-02 | 1.35E-07 |
| Quinoline | 6.63E-07 | 1.48 | 1.06E-02 | 2.20E-06 | 2-Cyclopenten-1-one, 3-methyl- | 1.73E-08 | 0.42 | 7.90E-03 | 4.27E-08 |
| 4H Cyclopenta[def]phenanthrene | 6.40E-07 | 1.49 | 1.56E-02 | 3.12E-06 | Propanoic acid, anhydride | 1.71E-08 | 0.47 | 1.07E-02 | 5.70E-08 |
| 2-Furanmethanol | 5.37E-07 | 1.76 | 8.07E-03 | 1.35E-06 | 5-tert-Butylpyrogallol | 1.70E-08 | 0.43 | 1.50E-02 | 7.93E-08 |
| 1,2-Benzenediol, 4-ethyl- | 4.96E-07 | 1.55 | 1.14E-02 | 1.76E-06 | Carbonocyanidic acid, ethyl ester | 1.66E-08 | 0.40 | 8.15E-03 | 4.22E-08 |
| Naphthalene, 2,6-diisopropyl- | 4.36E-07 | 1.38 | 1.75E-02 | 2.38E-06 | 2,3-Pentanedione | 1.26E-08 | 0.24 | 8.23E-03 | 3.23E-08 |
| Furfural | 4.35E-07 | 1.75 | 7.90E-03 | 1.07E-06 | 4H-Pyran-4-one | 1.14E-08 | 0.28 | 7.90E-03 | 2.80E-08 |

[A]Compositional mean values based on original mole fraction data (Eqn 3) sorted in descending order.
[B]Percentage of total (metric) variance (356.16) contributed by pyrolysate.
[C]Perturbation vector to convert mole fraction to mass fraction determined by closure of vector of molecular mass weights (Eqn 2).
[D]Mass fraction derived by perturbation of mole fraction values.

18.2% on a mole fraction basis and an additional 47.6% on a mass fraction basis. These eight compounds accounted for 99.6% and 98.8% on a mole and mass fraction basis, respectively. It is important to note that these are relative values based on the entire composition and that the previously reported values were calculated using different total mass or total number of moles for the PG and tars which makes comparison challenging as the terpene example illustrated.

The perturbation vector **p** (Table 4), which converts the composition from a mole basis to a mass basis, was formed by closure (Eqn 2) of the vector of molecular masses (Kim *et al.* 2019). The thermal decomposition of 1,2-benzenediol (catechol) has been studied in detail because it is a major structural entity of coal and a major component in biomass tars. Phenol is one of the major products of 1,2-benzenediol pyrolysis with maximum yield reported at 800°C (Ledesma *et al.* 2002; Thomas *et al.* 2007). These differences between mole and mass bases in the relative proportion that a specific part possesses serve as another example of the need to use statistical techniques that are not affected by an experimenter's choice of units to describe a composition (van den Boogaart and Tolosana-Delgado 2013). Although the mass fractions of CO and $H_2$ were quite dissimilar (Safdari *et al.* 2018), the mole fractions were the same order of magnitude. Note that these two gases also have similar high heats of combustion (–283 and –286 kJ $mol^{-1}$, respectively) (McCarty *et al.* 1981; DiNenno *et al.* 2002). In contrast, the mole fractions of $H_2$, phenol and $CO_2$ were similar, but the high heat of combustion of phenol was an order of magnitude larger than for $H_2$ (–3058 kJ $mol^{-1}$) (Cox 1961). Although the scale of the centre changes according to the fractional form chosen for the data, the log-ratio variances will not change, because of perturbation invariance. The preferred fractional form of the composition will likely change depending on how the data are used in various settings. The total (metric) variance (Eqn 5) for the pyrolysis data was 356.16 as obtained from the sum of the log-ratio variances of all pairs of parts of the composition. Smaller log-ratio variance indicates higher proportionality between parts. If the total variance is distributed equally between parts, the percentage contribution of each one would be 1/88 (1.1%). In our dataset, the PGs and phenol accounted for 0.17% of the total variance with the remainder in the other compounds ranging from 0.12% to 2.21%.

### *Effects of plant species, heating mode and moisture status*

The effects of the factors, plant species, heating mode and moisture status, are presented as follows. A global view of the significance of the effect of these factors is presented by the MANOVA. The analyses are then presented by factor. Pairwise comparisons between levels of each factor were performed. The effects of the factors on the designed balances are then presented in a combination of plots and pairwise comparisons. The results from the MANOVA and pairwise comparisons in this paper supersede the results presented previously (Safdari *et al.* 2019) for the following reasons. The analysis of variance previously used assumed that the response variable, gas concentration data (wt%), was (separately) normally distributed. This was inaccurate because proportions typically show a skewed profile individually and, fundamentally, in this case they are intrinsically interrelated to each other as parts of a composition. Hence, multivariate models such as the additive logistic normal distribution, the Dirichlet distribution or the log-ratio normal distribution (as resulting from considering *ilr* coordinates and assumed in this work) are in fact compatible probabilistic models (Mateu-Figueras *et al.* 2013). Second, it is well known that performing multiple comparisons via statistical significance testing results in Type I error (false positive or discovery) inflation. For example, there were 98 implied comparisons between the Slow and Conv heating modes using confidence intervals placed about mean yields of pyrolysis products in Safdari *et al.* (2019). Using eqn 6 from Jones (1984), the probability of one or more Type I errors occurring was $1 - (1 - 0.05)^{98} = 0.993$. In the present study, the Type I error rate for pairwise comparisons was properly controlled using the Benjamini and Hochberg's method that sets the expected proportion of false positives at the usual 5% level.

### *Global analysis*

Due to the lack of replication in the Rad treatment, it was not possible to estimate the three-way interaction term in the MANOVA applied to the *ilr*-transformed data. The very small *P* values associated with the global F-tests for plant species, moisture status and heating mode and all two-way interactions suggested that these factors significantly affected the mean values of the composition (Table 5). Because of scale and perturbation invariance, the results of the hypothesis tests in Table 5 do not change whether mole or mass fraction is used. Although the interaction terms were statistically significant, plots of marginal means (Fig. 1) suggested that only a few of the interaction terms were meaningfully different. Physical interpretation of this mean value was impossible, but the values can illustrate the fitted 'aggregate' or 'bulk' behaviour of the composition in response to the experimental factors. The heating modes were ordered by increasing heat flux in Fig. 1*a* and by the measured air temperature of the environment in Fig. 1*b*. It is

**Table 5. Multivariate analysis of variance testing significance of the effects of plant species, fuel moisture status and heating mode on pyrolysis gas composition**

| Source | d.f. | Pillai | *F* | num d.f. | den d.f. | *P* value |
|---|---|---|---|---|---|---|
| *Model with interactions* | | | | | | |
| Intercept | 1 | 1.00 | 11 437 829 | 87 | 127 | <0.0001 |
| Plant species | 14 | 14.00 | 41 325 | 1218 | 1960 | <0.0001 |
| Moisture status | 1 | 1.00 | 952 | 87 | 127 | <0.0001 |
| Heating mode | 3 | 3.00 | 698 183 | 261 | 387 | <0.0001 |
| Species*Status | 13 | 11.55 | 13 | 1131 | 1807 | <0.0001 |
| Species*Heating | 42 | 40.45 | 50 | 3654 | 7056 | <0.0001 |
| Status*Heating | 3 | 2.83 | 25 | 261 | 387 | <0.0001 |
| Residuals | 213 | | | | | |
| *Model with main effects only* | | | | | | |
| Intercept | 1 | 1.00 | 4 894 914 | 87 | 185 | <0.0001 |
| Plant species | 14 | 12.89 | 27 | 1218 | 2772 | <0.0001 |
| Moisture status | 1 | 0.90 | 20 | 87 | 185 | <0.0001 |
| Heating mode | 3 | 3.00 | 136 929 | 261 | 561 | <0.0001 |
| Residuals | 271 | | | | | |

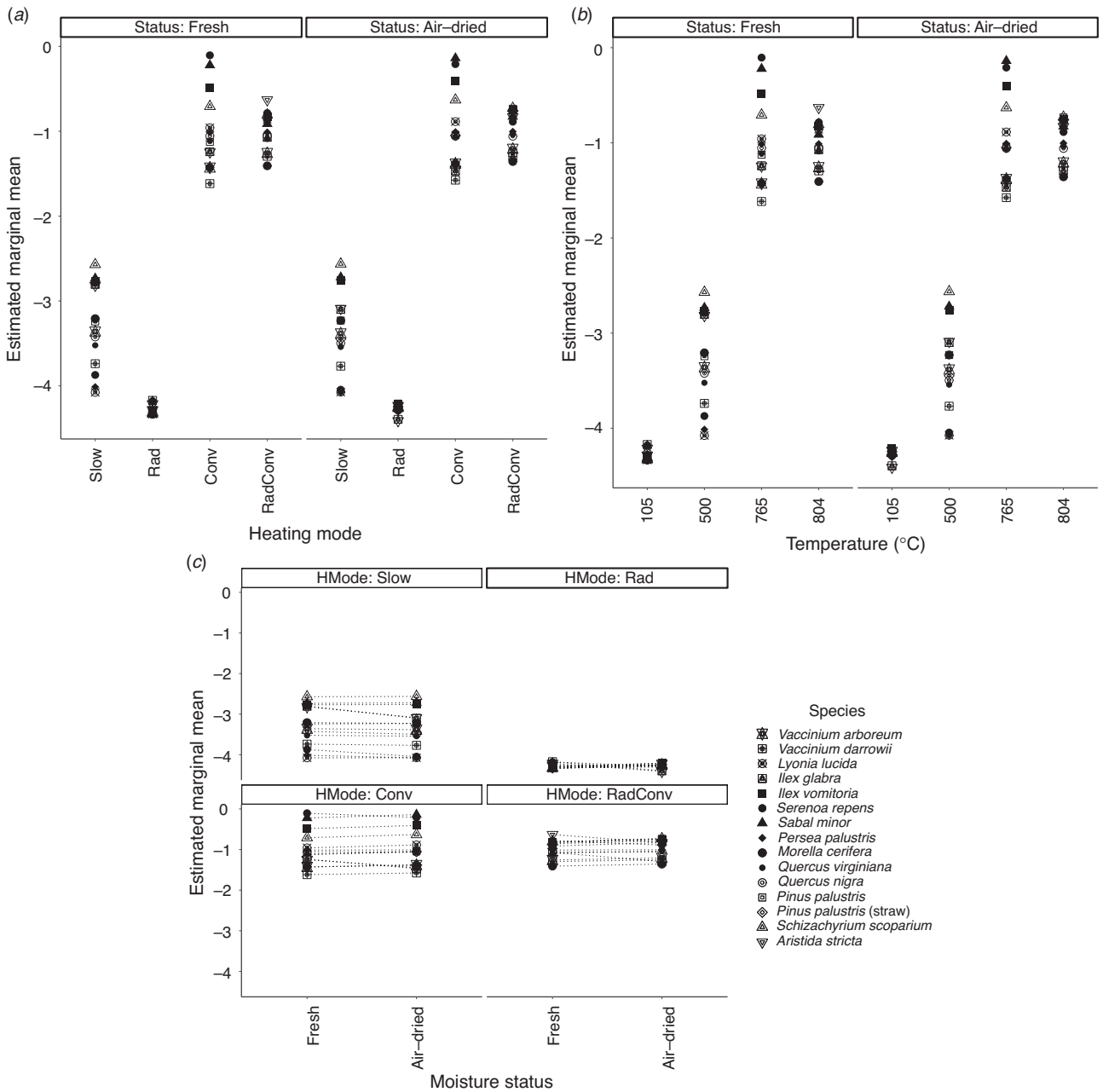


**Fig. 1.** Plots of estimated marginal means for effects of plant species, moisture status and heating mode on pyrolysis gas composition. Estimated marginal means arranged by (*a*) heating mode, (*b*) nominal temperature of heating mode environment and (*c*) moisture status. Marginal mean value for each plant species within a particular heating mode and moisture status combination calculated from the 87 balances resulting from an 88-part composition of pyrolysis gases. Conv, convective; Rad, radiant.

easily seen that both the heat flux and environmental temperature had a significant effect on the composition, which is consistent with our prior non-compositional analyses and the literature. The range in estimated marginal mean values for the plant species effect also changed for the different heating modes.

### *Heating mode*

The estimated mean effects for heating mode showed some general trends between heating modes (Fig. 2) across the individual gases. Here the effects are expressed as an average deviation (Eqn (7)), which is in log-ratio scale; the ratio of the effect geometric mean to the overall geometric can be calculated as *exp*(average deviation). For average deviations of –0.2, 0 and 0.2, the ratios of the geometric means are 0.82, 1 and 1.22. The average deviations for $H_2$, CO, $CO_2$, $CH_4$ and phenol were generally less than |0.2| for the heating modes, indicating that the ratios of the geometric means ranged within 80% to 120% of the overall mean (Fig. 2). Definite trends in the effects of heating

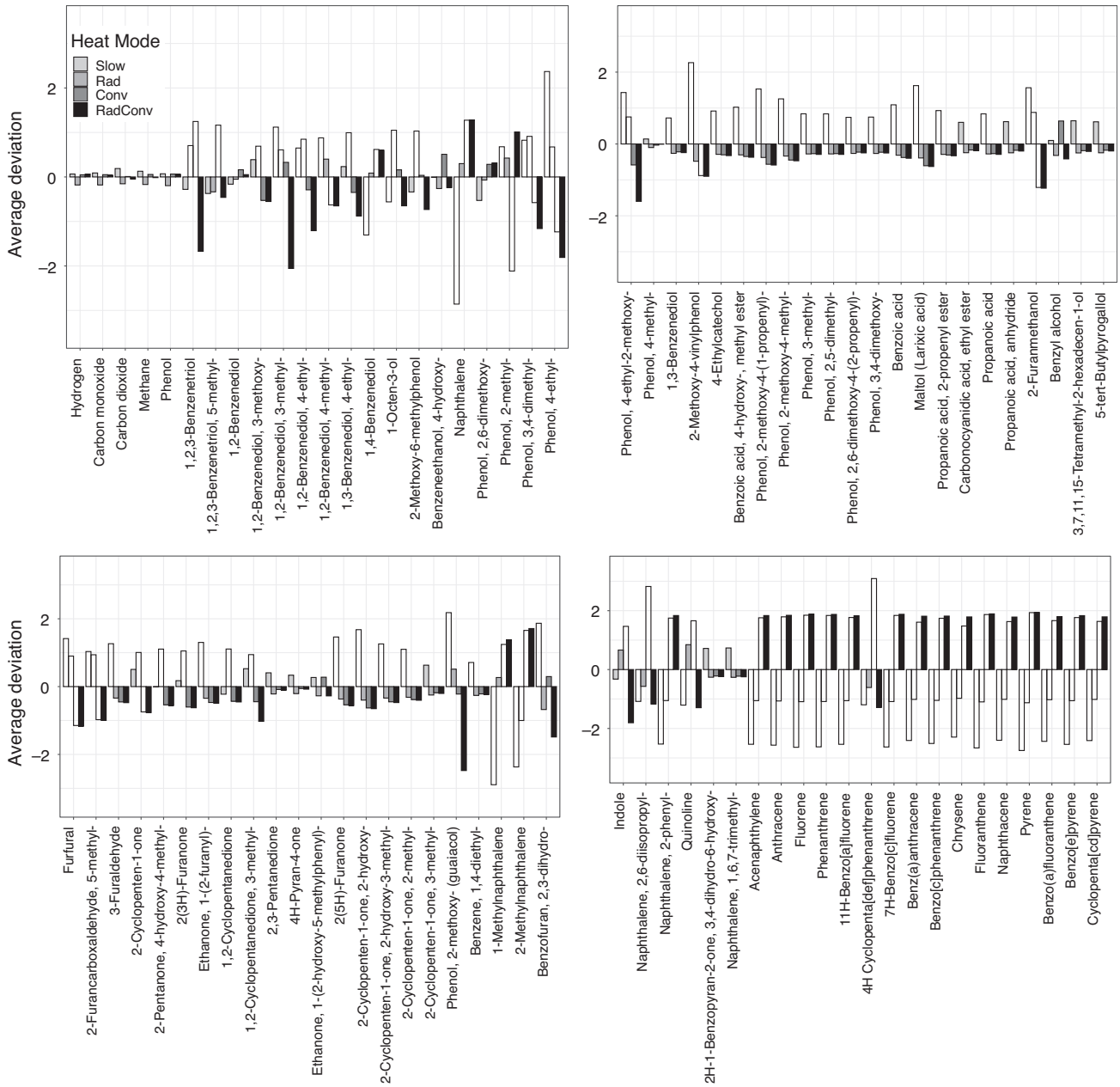


**Fig. 2.** Effect of heating mode on pyrolysis gas composition expressed as average deviation (log-ratio scale, Eqn 7) from overall geometric mean. Values below zero represent average mole fractions lower than overall value and values above zero represent the opposite.

mode on the relative amount of gases can be seen. For over 20 of the compounds, the average deviation for the Slow heating mode was positive while the other three modes were negative, indicating that the Slow heating mode produced relatively more of these gases. For 16 of the gases, the Slow and Rad modes had negative average deviations while the two higher heating modes, Conv and RadConv, had positive average deviations, meaning that relatively more of these compounds were produced at the higher heating rates. As discussed in Safdari *et al.* (2019), higher heating rates and increased pyrolysis temperatures increase tar and gas yields up to a maximum at which point the tars then decompose into light gases. Fig. 2 shows that the effect of heating rate on the composition of pyrolysis gases is complex: some gases increased while others decreased. Further analysis could be performed to group the gases by heating rate to ultimately seek a physical/chemical model describing the composition of pyrolysis gases. Such a detailed analysis was beyond the scope of this study.

The balances (Table 3) provided additional insight into the effects of heating mode on the pyrolysis products (Fig. 3). For the three balances involving the PGs, eight of the nine (three balances × three pairwise comparisons) differences between the Slow heating mode and the three FFB modes were positive and significant (Table 6). This means that the FFB modes

produced more tars relative to PGs, more CO relative to $H_2$, $CO_2$ and $CH_4$ and more $H_2$ relative to $CH_4$. Within the FFB results, the Conv mode produced more tars relative to PG compared with Rad and RadConv. RadConv produced the most CO relative to the other PG. The Slow mode produced the least amount of $H_2$ relative to $CH_4$ compared with the higher heating rates of the FFB; it also produced relatively less tar than phenol for Rad and Conv. The combined mode (RadConv) produced relatively less tar than phenol compared with Rad and Conv modes alone. The amount of phenol relative to the other tars did not differ between the pyrolyser (Slow) and the RadConv heating modes nor did it differ between Rad and Conv modes singly. Ledesma *et al.* (2002) reported maximum yield of phenol produced by the pyrolysis of 1,2-benzenediol at 800°C, the yield of benzene and 2–8-ring polyaromatic hydrocarbons began to increase at 700°C, which would decrease the amount of phenol relative to other tars. Recall that the gas temperatures of the four modes were 105°C for Rad and 500–800°C for Slow, Conv and RadConv.

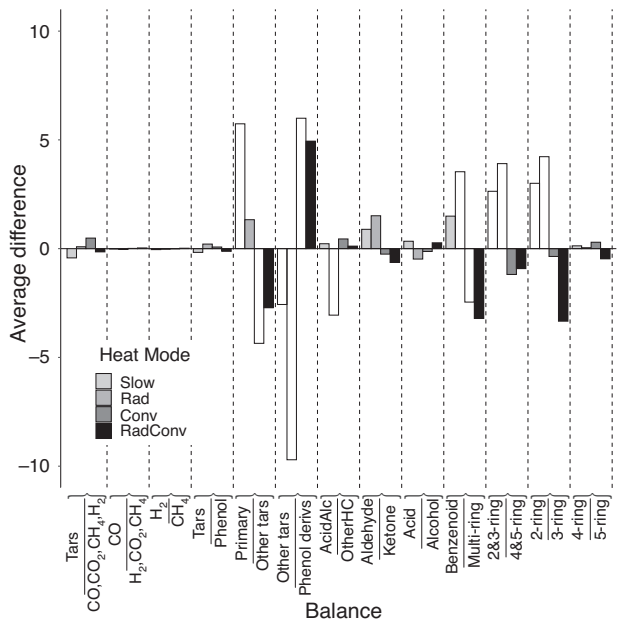


**Fig. 3.** Effect of heating mode on selected balances of pyrolysis gases. Displayed for each balance is the difference between mean value for heating mode and overall mean value. Values less than 0 indicate relatively less in the numerator; positive values, vice-versa. Conv, convective; Rad, radiant.

As the heating rate increased, lower amounts of primary tars were produced relative to other tars (negative differences for all pairwise comparisons except RadConv – Conv). For the FFB modes, the Rad mode produce the greatest amount of primary tars relative to other tars (excluding phenol), which decreased as environmental temperature (but not heat flux) increased. Several authors report an increase in tar production as temperature increases followed by a reduction, with an increase in gas products due to cracking of the tars (e.g. Fagbemi *et al.* 2001). This behaviour may explain the increase in the relative amount of tar to gas followed by a decrease in the FFB apparatus for these high heating rates. Similarly, increased heating rate produced relatively less benzenoid compounds relative to the multi-ring tars and generally smaller quantities of 3-ring tars relative to 2-ring tars. It is important to note that in Fig. 3 heating mode is ordered by the heat flux and not the environmental temperature as in Fig. 1*b*. This confirms that both the heating rate and the environmental temperature at which pyrolysis occurs are important factors that influence the composition of pyrolysis products.

When the ring compounds are considered, the pyrolyser generally produced smaller ring compounds, as indicated by more benzenoid (single ring) relative to multi-ring, more 2- and 3-ring compounds relative to 4- and 5-ring compounds and more 2-ring relative to 3-ring compounds. In contrast, the FFB modes

**Table 6. Pairwise comparison of heating mode and moisture status effects on balances of gas compounds produced by the pyrolysis of 15 plant species native to the south-eastern United States**

Values are pairwise difference and adjusted *P* value (Benjamini and Hochberg 1995). *P* value of 0.00 indicates *P* value < 1E-05. Shading indicates *P* value > 0.05. Conv, convective; HC, hydrocarbons; PG, permanent gas; Rad, radiant

| | Heating mode | | | | | | Moisture |
|---|---|---|---|---|---|---|---|
| Balance[A] | Rad–Slow | Conv–Slow | RadConv–Slow | Conv–Rad | RadConv–Rad | RadConv–Conv | Air-dried–Fresh |
| Tars vs PG | 2.29(0.00) | 3.03(0.00) | 0.92(0.00) | 0.74(0.00) | –1.37(0.00) | –2.11(0.00) | –0.02(0.86) |
| CO vs other PG | 0.01(0.57) | 0.15(0.00) | 0.22(0.00) | 0.14(0.00) | 0.21(0.00) | 0.07(0.00) | –0.06(0.00) |
| $H_2$ vs $CH_4$ | 0.07(0.03) | 0.13(0.00) | 0.34(0.00) | 0.05(0.09) | 0.26(0.00) | 0.21(0.00) | –0.19(0.00) |
| Tars vs phenol | 1.27(0.00) | 1.32(0.00) | 0.16(0.16) | 0.05(0.73) | –1.11(0.00) | –1.16(0.00) | 0.18(0.03) |
| Primary vs other tars | –5.82(0.00) | –33.64(0.00) | –28.19(0.00) | –27.82(0.00) | –22.37(0.00) | 5.46(0.00) | 0.09(0.89) |
| Other tars vs phenol derivatives | –6.68(0.00) | 45.65(0.00) | 42.14(0.00) | 52.33(0.00) | 48.82(0.00) | –3.51(0.00) | 0.03(0.94) |
| Acid, alcohol vs other HC | –10.94(0.00) | 0.73(0.05) | 0.40(0.29) | 11.68(0.00) | 11.34(0.00) | –0.33(0.34) | 0.16(0.56) |
| Aldehyde vs ketone | 2.08(0.00) | –5.49(0.00) | –5.08(0.00) | –7.57(0.00) | –7.16(0.00) | 0.41(0.35) | 0.04(0.91) |
| Acid vs alcohol | –5.93(0.00) | –1.57(0.00) | –0.23(0.66) | 4.36(0.00) | 5.69(0.00) | 1.34(0.01) | –0.26(0.53) |
| Benzene vs rings | –3.16(0.00) | –23.14(0.00) | –25.63(0.00) | –19.98(0.00) | –22.47(0.00) | –2.50(0.00) | 0.18(0.57) |
| 2- and 3- vs 4- and 5-ring | 4.24(0.00) | –12.74(0.00) | –17.96(0.00) | –16.98(0.00) | –22.20(0.00) | –5.22(0.00) | –0.05(0.86) |
| 2- vs 3-ring tars | 4.08(0.00) | –13.60(0.00) | –21.13(0.00) | –17.68(0.00) | –25.21(0.00) | –7.53(0.00) | –0.06(0.82) |
| 4- vs 5-ring tars | 0.00(1.00) | 0.55(0.00) | –1.99(0.00) | 0.55(0.00) | –1.99(0.00) | –2.54(0.00) | –0.01(0.83) |

[A]Balances defined in Table 3.

produced much less benzenoid relative to multi-ring. The Rad mode produced more 2- and 3-ring relative to 4- and 5-ring and more 2-ring relative to 3-ring. However, the Conv and RadConv modes produced much less benzenoid relative to the multi-ring tars, much less 2- and 3-ring relative to 4- and 5-ring and much less 2-ring relative to 3-ring. Recall that these relative ratios change whenever the numerator or the denominator of the balance changes. These results related to heating modes and pyrolysis gas composition, in agreement with many of the results presented in the original papers, are based on statistical tests and methodology that are appropriate to the nature of the data. As such, the results will not change if a subset or superset of the data are analysed, which was not the case for our original work.

### *Moisture status*

Only three of the 13 balances were affected by moisture (Table 6). The air-dried samples produced less CO relative to the other PGs, less $H_2$ relative to $CH_4$ and more tars relative to phenol. Moisture did not affect the amount of tar produced relative to PG nor did it affect any of the other balances. The mean moisture content of the fresh foliage ranged from 85% to 217% (Safdari *et al.* 2018), while the air-dried foliage moisture content ranged from 4% to 10% (Safdari *et al.* 2018; Amini *et al.* 2019). During the heating of the samples, the $H_2O$ evaporated and would have been part of the composition of measured gases; however, anhydrous $CaSO_4$ removed it so it was not possible to determine if its relative amount would have differed between the two moisture categories (Safdari *et al.* 2018). As the samples were aggregated over time, it was not possible to describe the temporal evolution of the gas composition. Instrumentation such as Fourier Transform Infrared (FTIR) spectrometers and quantum-cascade lasers can describe the evolution of the composition over time to determine the temporal dynamics of $H_2O$ in the processes leading up to ignition. Previous modelling of the effect of moisture on the ignition of gas mixtures has shown that ignition can occur even when a relatively large amount of $H_2O$ is present (Ferguson *et al.* 2013). Although typically not reported in smoke emission studies, the amount of water vapour in the pyrolysis gas composition can be estimated using various FTIR instruments (e.g. Scharko *et al.* 2019*a*; Phillips *et al.* 2020). The lack of $H_2O$ in the pyrolysis gas composition did not affect the results for the other gas ratios due to subcompositional coherence, which would not have been the case if $H_2O$ were included in the prior analysis that used standard correlation and other methods based on this.

### *Plant species*

Average deviation plots of the plant species effects were quite complex and not easily interpreted. They are included as Supplemental Material. Results for the eight dominant parts of the pyrolysis gas composition (Table 4) are presented here. The average deviation changed appreciably by plant species (Fig. 4). The eight dominant gases provide a contrast in the consistency of the effect of plant species. For the PGs (Fig. 4), the range of average deviations were relatively small (–0.03 to 0.03, which equates to 97–102% of the overall mean) for all of the plant species, indicating that the geometric mean of each plant species was close to the overall mean. From Eqn 7, the average deviation can be converted to a percentage as 100*exp*(average deviation). *Vaccinium arboreum*, *V. darrowii*, and *Morella cerifera* consistently produced relatively less of the PGs ($H_2$, CO, $CO_2$, $CH_4$) (average deviation $< 0$) than the other plant species, while *Ilex vomitoria*, the palmettos *Serenoa repens* and *Sabal minor* and the grass *Schizachyrium scoparium* produced relatively more. Bear in mind that the range in average deviation was only 5% for the PGs. Trends in the four most dominant tars were not as readily apparent. The range in average deviation for phenol was comparable to that for the PGs (–0.04 to 0.06), but much larger for the remaining three (–0.30 to 0.13), which equates to 74–114% of the overall mean. The average deviation for *S. scoparium* was consistently less than 0 for the four tars. No other consistent trends were noted for the four dominant tars. For the full set of gases, the average deviation ranged from –0.58 to 0.59, which is equivalent to 55–180% of the overall mean. Various multivariate methods could be applied to the log-ratios to cluster plant species based on the relative composition of the pyrolysis gases, but this was beyond the scope of the present study.

The effects of plant species on the selected gas species balances were somewhat more consistent (Table 7, Fig. 5). These figures present the average effect (difference between the arithmetic mean value of a balance for a plant species and the overall arithmetic mean value of the balance). Pairwise comparisons of the average effects (differences) between species identified similarities in pyrolysis composition between some species (Table 7). A total of 1365 (15 species × 13 balances) pairwise comparisons were performed. For a balance, plant species followed by the same letter were not statistically different based on *t*-tests with the *P* value adjusted to control for false discovery rate. Fig. 5 presents the average effects grouped by gas species balance and Fig. 6 presents the differences grouped by plant species. The relative magnitude and sign (+, −) of the average effect for each plant species is shown in Fig. 5 and Fig. 6. Although in Fig. 5 it appears that plant species had little effect on the two balances involving the PGs, because the average effects were very close to 0, the pairwise comparisons between species indicated otherwise. Based on the pairwise comparisons (Table 7), *Serenoa repens*, *Sabal minor* and *Schizachyrium scoparium* produced similar amounts of tar relative to PGs. The *Vacciniums* and three other species produced relatively more $H_2$ than $CH_4$. The amount of tars produced relative to phenol by *S. repens* and *S. minor* differed from all other species and were negative (Table 7, Fig. 5), indicating that the palmettos produced relatively more phenol than tars. The pairwise comparisons of the balances resulted in many different groupings of the plant species; however, the average deviations for many of the balances for *Ilex glabra*, *I. vomitoria*, *S. scoparium* and the palms *S. repens* and *S. minor* were negative suggesting similar relative amounts for many of the same balances (Fig. 6). A majority of average deviations for *Vaccinium arboreum*, *V. darrowii*, *Lyonia lucida*, *Persea palustris*, *Pinus palustris* litter and the oaks *Quercus nigra* and *Q. virginiana* were positive, indicating that the relative amounts of compounds in the balances for this group were different from *I. glabra*, *I. vomitoria*, *S. scoparium*, *S. repens* and *S. minor*.

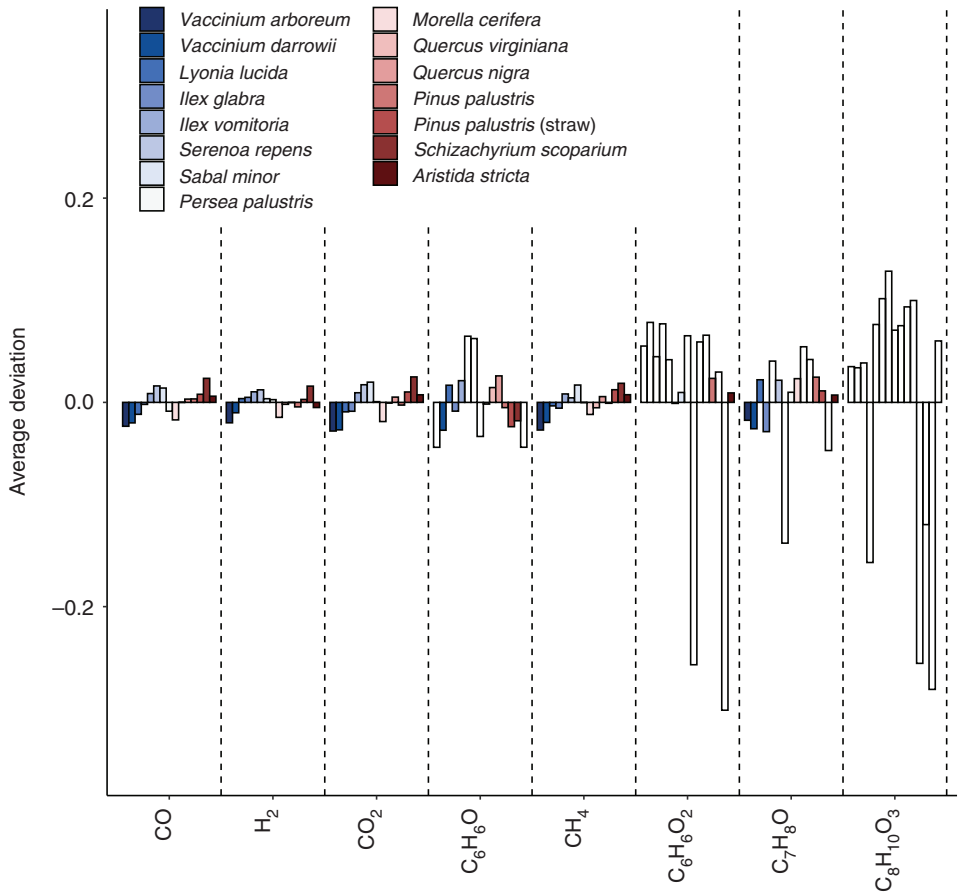


**Fig. 4.** Effect of plant species on estimated amount of top eight dominant pyrolysis gases. Values below zero represent effect lower than overall effect while values above zero represent the opposite. Vertical dotted lines segregate the plant effects for each gas.

**Table 7. Pairwise comparison of plant species effects on balances of gas compounds produced by the pyrolysis of 15 plant species native to the south-eastern United States**

For each balance, plant species that did not differ are indicated by the same letter. Means in ascending order. *P* values adjusted to control the false discovery rate at 0.05 (Benjamini and Hochberg 1995). Average effects for plant species are shown in Fig. 5 and Fig. 6. HC, hydrocarbons; PG, permanent gas

| Species | Tar vs PG | CO vs other PG | $H_2$ vs $CH_4$ | Tars vs phenol | Primary vs other tars | Other tars vs phenol derivatives | Acid and alcohol vs other HC | Aldehyde vs ketone | Acid vs alcohol | Benzenoid vs multi-ring | T23 vs T45 | T2 vs T3 | T4 vs T5 |
|---|---|---|---|---|---|---|---|---|---|---|---|---|---|
| *Vaccinium arboreum* | g | b efg | c e | e | bc e | a | c e | a | a c | e | d | c | bc |
| *Vaccinium darrowii* | cde | bc | e | bc | a | a | e | ab | a c | cd | bcd | a c | de |
| *Lyonia lucida* | d f | a | c e | b | a c | a | de | cd | ab | d | a | a c | bc |
| *Ilex glabra* | fg | b efg | e | cd | def | a | a c | a | bc | bcd | a d | a c | a |
| *Ilex vomitoria* | ef | b e | a c e | bc | f | bc | a | a d | d | e | a c | a c | a |
| *Serenoa repens* | a c | d g | de | a | bc e | ab | ab | cd | ab | a | a | a | ab |
| *Sabal minor* | a | b ef | b | a | ef | c | a | a c | a c | a | a d | a c | a |
| *Persea palustris* | fg | a | a c e | de | ab | a | bcd | a c | bc | de | cd | bc | c |
| *Morella cerifera* | cde | b | bcd | b | bcd | a | bcd | cd | a c | d | ab | a | d f |
| *Quercus virginiana* | f | cde | a c e | bc | ef | a | bcd | bcd | ab | a | cd | a c | fg |
| *Quercus nigra* | d f | b e | ab | b | ef | a | bcd | cd | a | a | a d | a c | efg |
| *Pinus palustris* | bcd | d | bc | b | c f | a | cd | bcd | cd | ab | a c | ab | g |
| *Pinus palustris* (*straw*) | d f | b de | ab | de | ef | a | bc e | bcd | cd | de | a | a | d f |
| *Schizachyrium scoparium* | ab | d f | bcd | bc | ef | c | de | a d | ab | a c | a d | a | fg |
| *Aristida stricta* | d f | de | b | de | bc e | a | a cd | d | ab | d | a | a c | cd |

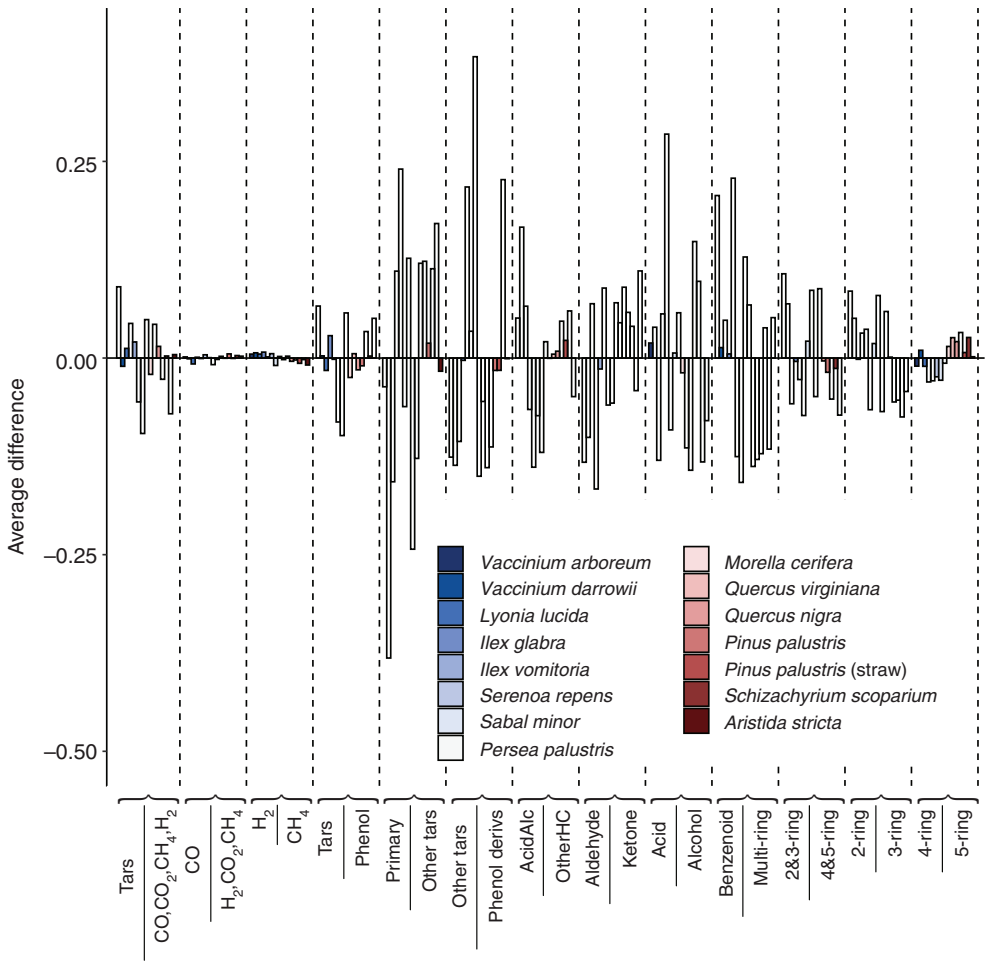


**Fig. 5.** Effect of plant species on selected balances of pyrolysis gases. Displayed for each balance is the difference between mean value for species and overall mean value. Values less than 0 indicate relatively less in the numerator; positive values, vice-versa.

The amount of primary tars relative to other tars produced by *V. darrowii*, *L. lucida* and *P. palustris* was significantly less than other plant species. At least eight of the 15 plant species did not differ for the primary tar balance. *Schizachyrium scoparium* and *S. minor* produced more of the secondary and tertiary tars relative to the phenol derivatives; 12 of the 13 remaining plant species produced similar amounts of these other tars relative to the phenol derivatives. The plant species appear to fall into two groups for the 2- and 3-ring tars versus the 4- and 5-ring tars; however, there was little difference in plant species for the 2- versus 3-ring tar balance. This grouping of plant species appeared to more influenced by differences in the relative amounts of 4-ring tars to 5-ring tars. Tars (condensable gases) are an important primary pyrolysis product that can undergo secondary pyrolysis yielding lighter gases and soot, which are important in combustion and heat transfer processes as well as being components of smoke that are often hazardous to human health. Other plant species groupings for other balances were identified but not highlighted here. Plant species are classified typically by easily seen characteristics such as flower structure, fruit type, leaf structure, etc. Closely related species and genera share common characteristics (such as the oaks, the palms, the grasses etc.). These similarities in physical and genetic characteristics translated to similarity in the composition of pyrolysis gases as expressed in the various balances. Generally, for the plant species within the same genus, the pairwise comparisons did not indicate that the species differed for many of the balances. However, the *Vacciniums* differed in the amount of tar produced relative to PGs as did the grasses. Similarly, the *Vacciniums* and grasses differed within each group in terms of the tar versus phenol balance.

CO, $CO_2$, $CH_4$, $H_2$ and phenol were the dominant pyrolysis products in all four heating modes; CO, $CH_4$ and $H_2$ readily combust. 1,2-benzenediol (catechol), which can pyrolyse into phenol, CO and $CH_4$ at the temperatures used in the present study (Ledesma *et al.* 2002) and phenol, which can pyrolyse into CO at the upper temperature range of the present study (Lovell *et al.* 1989), were significant components of the pyrolysis products and result from the decomposition of lignin (Jegers and Klein 1985). The pyrolysis pathways of these two products have been described and it may be possible to add these pathways to the pyrolysis scheme used in GPyro3D-FDS coupled

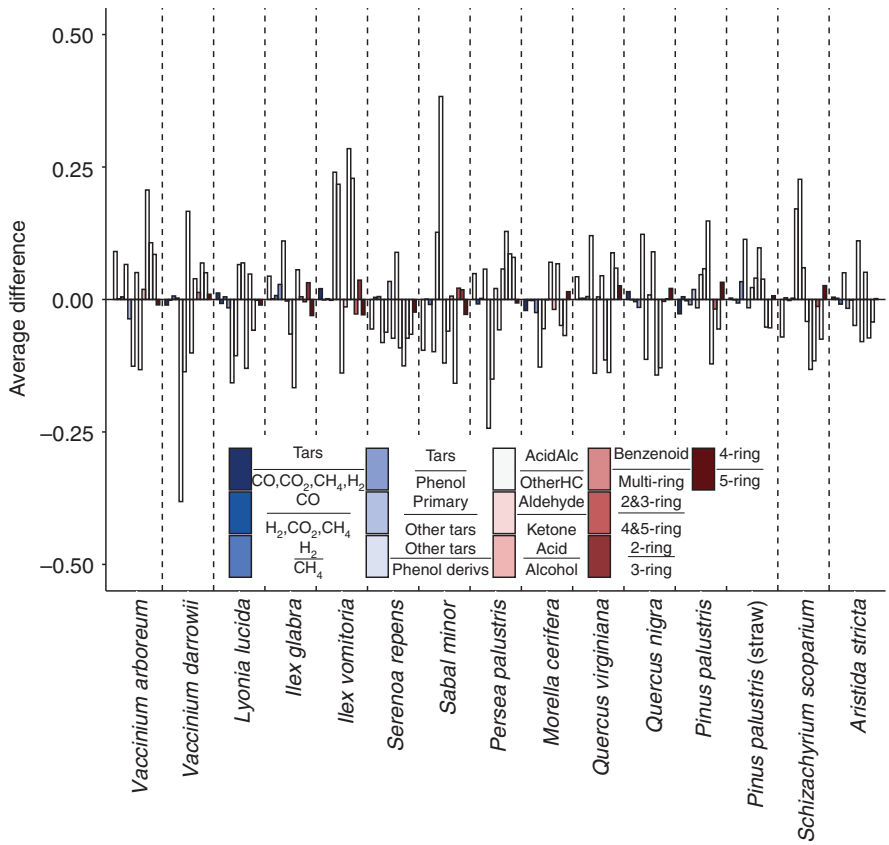


**Fig. 6.** Effect of plant species on selected balances of pyrolysis gases arranged by species. Displayed for each balance is the difference between mean value for species and overall mean value. Values less than 0 indicate relatively less in the numerator; positive values, vice-versa.

applications. The GPyro3D-FDS coupling currently includes water for high moisture content fuels and the extended Broido-Shafizadeh scheme (Di Blasi 1994; Yashwanth *et al.* 2016), which includes the breakdown of tars into lower molecular weight gases. It is unknown what kind of effect the addition of these specific mechanisms would have on ignition of live fuels or if the additional computational demand is justified.

In our prior combined analysis of the effect of heating mode on the composition of pyrolysis products, Safdari *et al.* (2020) observed large changes in tar composition between plant species, but no major changes in the types of compounds produced by pyrolysis between the fresh and dried samples. The present analysis identified how the mixture of pyrolysis products varied among species. By combining the individual gases into meaningful groups and examining the effect of plant species, moisture status and heating mode on the relative amounts of the groups produced during pyrolysis, it was possible to untangle some of the complexity of the multivariate data.

The analysis based on balances made readily apparent the dominance of the PGs relative to the tar compounds for both the slow and fast pyrolysis experiments. Of the 15 plant species, *Vaccinium arboreum* produced the most tar relative to the PGs. CO was the dominant PG produced; however, a greater number of moles of $H_2$ was produced relative to $CH_4$. If a ratio measure based on the absolute quantities of CO and $CO_2$, such as combustion efficiency or modified combustion efficiency (Ward *et al.* 1980; Ward and Hao 1991; Yokelson *et al.* 1997) described the experimental conditions, the dominance of CO would suggest that these experiments fell within the smouldering combustion regime, which is not logical because no combustion occurred. Combustion efficiency, a measure correlated with all other pyrolysis gases due to the relative nature of compositional data, should be used in a manner consistent with its relative and multivariate nature (Weise *et al.* 2020*b*).

The amount of $H_2$ relative to $CH_4$ varied between plant species and higher heating rates resulted in more $H_2$ relative to $CH_4$. Fast pyrolysis of biomass is preferred over slow pyrolysis for $H_2$ production (Ni *et al.* 2006); however, it is difficult to compare results because the data are not treated as compositional data. The implications of the amount of $H_2$ relative to $CH_4$ for modelling are currently unknown. The higher heating rates and temperatures of the FFB apparatus produced more tars relative to the PGs, which is consistent with the literature. Although the slow pyrolysis (pyrolyser) experiments led to the formation of nearly 300 compounds, only 20–25% of them were measured above detection limits enabling analysis. Of the 84 tars included in the present analysis, the relative amount of phenol compared with all other tars dominated the tar mixture. The relative amount of phenol differed between species and the higher heating mode experiments produced more tar relative to

phenol when compared with the slow-heating pyrolyser. To our knowledge phenol is not currently included in any pyrolysis mechanisms in the physically-based fire spread models (Colman and Linn 2007; Mell *et al.* 2009), but should be considered given its relative dominance. A framework to modify the thermal degradation of biomass based on summative analysis has been recently proposed (Dietenberger *et al.* 2020).

We previously reported that 1–5-ring aromatic compounds were major components in the FFB experiments (Safdari *et al.* 2020). The balance between primary tars and other tars confirmed this prior observation and showed that the amount of primary tars relative to the 1–5-ring compounds was very small for the convective and combined heating modes when compared with the slow-heating pyrolyser. The relative amount for the radiant heating mode only, while significantly smaller than the pyrolyser, was not as small as the other two FFB heating modes. Similarly, the benzenoid compounds (1-ring), although dominant relative to the multi-ring compounds in the slow-heating experiment, were much less dominant in the convective and combined heating modes. The current analysis showed that the relative amounts of pyrolysis products were strongly affected by both plant species and heating mode, which may explain observed differences in ignition and fire spread in these plant types. The moisture status did not have a strong effect on the composition of the non-$H_2O$ pyrolysis products, which supports the idea that the effect of fuel moisture content occurs due to dilution of the gas mixture by the addition of water vapour only (e.g. Catchpole and Catchpole 1991; Ferguson *et al.* 2013). However, the temporal dynamics of water vapour in the composition are still undescribed, even though recent progress in measurements is beginning to shed light on this (Tree *et al.* 2019; Phillips *et al.* 2020). Progress has been made in terms of improving the modelling of water vapour's role (Shotorban *et al.* 2018). Pyrolysis of cellulose begins in the vicinity of 320–340°C and other volatile compounds can be released at lower temperatures (e.g. Maleknia *et al.* 2009*a*, 2009*b*). All these products contribute to the overall composition of compounds released by the heating of wildland fuels and the temporal evolution of the composition remains to be described. Although the dominant pyrolysis products can be described as $H_2$, CO, $CO_2$, $CH_4$ and phenol, with a few other phenol-based derivatives, the practical effects of this simplified mixture on physically-based models will be unknown until we are able to incorporate this information into pyrolysis models that are linked to fire behaviour models to test the sensitivity of the model to pyrolysis gas composition.

The comparison of results in the present analysis with our prior results (Table 8) is challenging because many of our previous conclusions were based on discerning trends in simple statistical tests that may or may not have been correctly applied. Many of the results in the present analysis agree with previous conclusions. The observed trends of heating mode effects on pyrolysate composition previously identified were corroborated with the present analysis. However, it was possible to perform pairwise comparisons of different balances of the pyrolysates and identify where the plant species were similar and where they differed. Similarly, the effects of plant moisture content and heating mode on the different balances provided more information than previously extracted from the data. Further exploration and modelling of the data using the full complement of statistical tools based on 'traditional' methods is now possible after applying CoDA methodology to ensure that the data better meet the statistical assumptions underlying the methods.

## Conclusions

The data describing the composition of gas mixtures such as pyrolysis products and smoke emissions are inherently multivariate and relative in nature. Although this has been recognised for many years, the statistical techniques commonly used to analyse the data ignore these features. This not only applies to gas mixtures, but also to the composition of the product yields associated with different heating rates, which we did not analyse here (Safdari *et al.* 2018, 2019, 2020; Amini *et al.* 2019), as well as the composition of the different fuel types that pyrolyse to produce the products and then combust to produce a myriad of gaseous and solid emissions. Because pyrolysates, smoke emissions and fuel composition represent parts of a whole, the measured values of the individual parts (elements, chemical species, fuel components etc.) are intrinsically not independent from each other. The measured values are relative and are only meaningful in relation to each other. Such constraints violate many of the underlying assumptions of ordinary statistical methods. Compositional data analysis is a well-developed body of statistical methodology that provides models and methods equivalent to traditional ones while accounting for these special constraining features of relative data. The expression of pyrolysis data as ratio data such as mole fractions or mass fractions has long been reported. We have shown that these different ratios are simply a change of units that does not change the underlying variability of the relative data, which is important from a statistical hypothesis-testing perspective.

The use of compositional balances to form log-ratios contrasting subsets of parts of interest enabled hypothesis testing to examine relative differences in the amounts of gaseous pyrolysis products caused by plant species, moisture content and heating mode. The results of this hypothesis testing have more formal rigour than was previously presented, by respecting the very relative nature of the data. We have definitively shown that plant species affected several different ratios of groups of pyrolysates and are assured that the results are not an artefact of the analysis, which can then be used to make various inferences and decisions. The effects of heating mode, which was confounded with heating rate, were shown to definitively affect the composition of pyrolysis products and we are assured that these results are not an artefact of the analysis. Increased heating rate resulted in less primary tars relative to other tars; the radiation-only mode, which also had the lowest environmental temperature, produced the greatest amount of primary tars relative to other tars. The higher heating rates also produced more $H_2$ relative to $CH_4$. The production of phenol relative to tars was more complex. The pyrolyser and the FFB combination of radiation and convection, which represented the lowest and highest heating rates, produced less tar relative to phenol than radiant and convective heating alone, which represented the intermediate heating rates. The relative amounts of the pyrolysis products did not differ between fresh and air-dried samples. The presence of $H_2O$ in the samples would not affect the ratios between the other gases, suggesting

**Table 8. Comparison of results from 'traditional' statistical methods and current compositional data approach**

Conv, convective; PG, permanent gas; Rad, radiant

| Analysis | This paper | (Safdari *et al.* 2018) (fast) | (Amini *et al.* 2019) (slow) | (Safdari *et al.* 2019) (slow vs fast) | (Safdari *et al.* 2020) (radiative vs convective) |
|---|---|---|---|---|---|
| Tar composition by plant species | • Plant species, heating mode and live vs air-dried all significantly affected composition<br>• 1 grass, sparkleberry, longleaf pine had highest tar relative to phenol<br>• Many groupings of pyrolysates differed between plant species<br>• Non-primary tars relative to phenol derivatives not affected by most plant species | • Some large changes between species<br>• Grasses and longleaf pine had lowest phenol concentrations<br>• Distribution of functional groups differed between species<br>• 1–5-ring tars observed | • Plant species more important than live vs air-dried<br>• Significant difference in distribution of tar functional groups<br>• Few multiple-ring tars observed | | |
| Composition of fresh and air-dried | • Live had more CO relative to $CO_2$, $CH_4$, $H_2$<br>• Live had more $H_2$ relative to $CH_4$<br>• Air-dried produced more phenol relative to other tars | • CO main component<br>• No major changes in types observed<br>• Some species differed in light gases<br>• CO, $H_2$ slightly higher in live, $CO_2$, $CH_4$ slightly higher in air-dried<br>• Small difference in tar functional groups | • No difference in distribution of tar functional groups<br>• CO, $H_2$ slightly higher in live, $CO_2$, $CH_4$ slightly higher in air-dried<br>• Differences in fire behaviour should be due to moisture and not pyrolysis products | | |
| Slow vs fast heating | • Numerous significant comparisons between all heating modes for ratios of groups of compounds | | | • Higher yield of CO in fast, higher yield of $CO_2$ in slow<br>• More multi-ring tars in fast pyrolysis<br>• Phenol observed in fast heating | |
| Tar yield | • Rad and Conv, but not RadConv produced more tar relative to phenol than slow heating<br>• RadConv produced less tar relative to phenol than Rad and Conv alone | | | | • Tar yield increased with temperature in fast experiments |

(*Continued*)

**Table 8. (Continued)**

| Analysis | This paper | (Safdari *et al.* 2018) (fast) | (Amini *et al.* 2019) (slow) | (Safdari *et al.* 2019) (slow vs fast) | (Safdari *et al.* 2020) (radiative vs convective) |
|---|---|---|---|---|---|
| Composition | • Fast heating produced less primary tars relative to slow heating<br>• RadConv produced relatively more primary tars relative to multi-ring than Conv<br>• Several higher heating rates produced more multi-ring relative to phenol derivatives | | | | • Lowest CO in Rad, highest in RadConv<br>• $CO_2$ percentage decreased with temperature and heating rate<br>• Mostly primary tars in Rad<br>• Conv, RadConv more multi-ring tars<br>• Principal tars (phenol, 1,2-benzenediol varied widely between plant species; no clear general trend with heating mode |
| All parts of composition analysed together | Yes, mole% (comparison results independent of basis) | PG and tars separately, wt% and mole% | PG and tars separately, wt% and mole% | PG and tars separately, wt% and mole% | PG and tars separately, wt% and mole% |
| Type I error rate | Controlled | Uncontrolled | Uncontrolled | Uncontrolled | Uncontrolled |
| Spurious correlation results? | Not possible | Possible | Possible | Possible | Possible |
| Confidence intervals $< 0$? | Not possible | Possible | Possible | Possible | Possible |

water's role may only be as a diluent. It is important to note that the effects of plant species, heating mode and moisture status are independent of the units used to describe the composition due to the use of CoDA. The only difference is found in the value of the intercept term, which reflects the translation of the data expressed in real-valued *ilr* coordinates derived from the change of units by perturbation. More complex analyses of log-ratios of gas pairs or groupings as functions of heating rate are possible. We recommend that future analysis of the composition of pyrolysis products, smoke emissions, fuel composition and other data related to wildland fire that are compositional in nature be performed using CoDA techniques to provide more statistically rigorous and consistent results. These results show the wide variety in the composition of the tar products produced by these plant species in relatively small amounts; however, the oxidation of these products by combustion and transformation by other plume and atmospheric processes produces the wide variety of trace gases associated with wildland fire.

## Conflicts of interest

The authors declare no conflicts of interest.

## Declaration of funding

JPA was partly supported by the Scottish Government's Rural and Environment Science and Analytical Services Division and the Spanish Ministry of Science, Innovation and Universities (CODAMET RTI2018-095518-B-C21, 2019–2021).

## Acknowledgements

The data used in this paper resulted from the DOD/DOE/EPA Strategic Environmental Research and Development Program project RC-2640 and will be archived in the USDA Forest Service Research Data Archive (https://www.fs.usda.gov/rds/archive/). The use of trade or firm names in this publication is for reader information and does not imply endorsement by the US Department of Agriculture of any product or service.

## References

Aitchison J (1986) 'The statistical analysis of compositional data.' (Chapman and Hall: London)

Aitchison J (2003) A concise guide to compositional data analysis. Available at http://ima.udg.edu/activitats/codawork03/

Aitchison J, Egozcue JJ (2005) Compositional data analysis: where are we and where should we be heading? *Mathematical Geology* **37**, 829–850. doi:10.1007/S11004-005-7383-7

Aitchison J, Barceló-Vidal C, Martín-Fernández JA, Pawlowsky-Glahn V (2000) Logratio analysis and compositional distance. *Mathematical Geology* **32**, 271–275. doi:10.1023/A:1007529726302

Akagi SK, Yokelson RJ, Wiedinmyer C, Alvarado MJ, Reid JS, Karl T, Crounse JD, Wennberg PO (2011) Emission factors for open and domestic biomass burning for use in atmospheric models. *Atmospheric Chemistry and Physics* **11**, 4039–4072. doi:10.5194/ACP-11-4039-2011

Aminfar A, Cobian-Iñiguez J, Ghasemian M, Rosales Espitia N, Weise DR, Princevac M (2020) Using background-oriented schlieren to visualize convection in a propagating wildland fire. *Combustion Science and Technology* **192**, 2259–2279. doi:10.1080/00102202.2019.1635122

Amini E, Safdari M-S, DeYoung JT, Weise DR, Fletcher TH (2019) Characterization of pyrolysis products from slow pyrolysis of live and dead vegetation native to the southern United States. *Fuel* **235**, 1475–1491. doi:10.1016/J.FUEL.2018.08.112

Andreae MO, Merlet P (2001) Emission of trace gases and aerosols from biomass burning. *Global Biogeochemical Cycles* **15**, 955–966. doi:10.1029/2000GB001382

Andreae MO, Browell EV, Garstang M, Gregory GL, Harriss RC, Hill GF, Jacob DJ, Pereira MC, Sachse GW, Setzer AW, Dias PLS, Talbot RW, Torres AL, Wofsy SC (1988) Biomass-burning emissions and associated haze layers over Amazonia. *Journal of Geophysical Research* **93**, 1509–1527. doi:10.1029/JD093ID02P01509

Banach CA, Bradley AM, Tonkyn RG, Williams ON, Chong J, Weise DR, Myers TL, Johnson TJ (2021) Dynamic infrared gas analysis from longleaf pine fuel beds burned in a wind tunnel: observation of phenol in pyrolysis and combustion phases. *Atmospheric Measurement Techniques* **14**, 2359–2376. doi:10.5194/AMT-14-2359-2021

Bandeen-Roche K (1994) Resolution of additive mixtures into source components and contributions: a compositional approach. *Journal of the American Statistical Association* **89**, 1450–1458. doi:10.1080/01621459.1994.10476883

Barceló-Vidal C, Martín-Fernández J-A (2016) The mathematics of compositional analysis. *Austrian Journal of Statistics* **45**, 57. doi:10.17713/AJS.V45I4.142

Barceló-Vidal C, Martín-Fernández JA, Pawlowsky-Glahn V (2001) Mathematical foundations of compositional data analysis. In'Proceedings of IAMG '01, Cancun, MX'. (Ed. G Ross) pp. 1–20. (International Association for Mathematical Geosciences: Cancun, MX). Available at http://ima.udg.edu/~barcelo/index_archivos/Cancun.pdf.

Benjamini Y, Hochberg Y (1995) Controlling the false discovery rate: a practical and powerful approach to multiple testing. *Journal of the Royal Statistical Society. Series B. Methodological* **57**, 289–300. doi:10.1111/J.2517-6161.1995.TB02031.X

Billheimer D (2001) Compositional receptor modeling. *Environmetrics* **12**, 451–467. doi:10.1002/ENV.472

Buccianti A, Pawlowsky-Glahn V (2006) Statistical evaluation of compositional changes in volcanic gas chemistry: a case study. *Stochastic Environmental Research and Risk Assessment* **21**, 25–33. doi:10.1007/S00477-006-0041-X

Butler BW, Cohen J, Latham DJ, Schuette RD, Sopko P, Shannon KS, Jimenez D, Bradshaw LS (2004) Measurements of radiant emissive power and temperatures in crown fires. *Canadian Journal of Forest Research* **34**, 1577–1587. doi:10.1139/X04-060

Butler B, Teske C, Jimenez D, O'Brien J, Sopko P, Wold C, Vosburgh M, Hornsby B, Loudermilk E (2016) Observations of energy transport and rate of spreads from low-intensity fires in longleaf pine habitat – RxCADRE 2012. *International Journal of Wildland Fire* **25**, 76–89. doi:10.1071/WF14154

Butler BM, Palarea-Albaladejo J, Shepherd KD, Nyambura KM, Towett EK, Sila AM, Hillier S (2020) Mineral–nutrient relationships in African soils assessed using cluster analysis of X-ray powder diffraction patterns and compositional methods. *Geoderma* **375**, 114474. doi:10.1016/J.GEODERMA.2020.114474

Catchpole EA, Catchpole WR (1991) Modelling moisture damping for fire spread in a mixture of live and dead fuels. *International Journal of Wildland Fire* **1**, 101–106. doi:10.1071/WF9910101

Collard F-X, Blin J (2014) A review on pyrolysis of biomass constituents: mechanisms and composition of the products obtained from the conversion of cellulose, hemicelluloses and lignin. *Renewable & Sustainable Energy Reviews* **38**, 594–608. doi:10.1016/J.RSER.2014.06.013

Colman JJ, Linn RR (2007) Separating combustion from pyrolysis in HIGRAD/FIRETEC. *International Journal of Wildland Fire* **16**, 493–502. doi:10.1071/WF06074

Cox JD (1961) The heats of combustion of phenol and the three cresols. *Pure and Applied Chemistry* **2**, 125–128. doi:10.1351/PAC196102010125

Crutzen PJ, Heidt LE, Krasnec JP, Pollock WH, Seiler W (1979) Biomass burning as a source of atmospheric gases $CO$,$H_2$, $N_20$, NO, $CH_3Cl$ and COS. *Nature* **282**, 253–256. doi:10.1038/282253A0

Di Blasi C (1994) Numerical simulation of cellulose pyrolysis. *Biomass and Bioenergy* **7**, 87–98. doi:10.1016/0961-9534(94)00040-Z

Di Blasi C (2008) Modeling chemical and physical processes of wood and biomass pyrolysis. *Progress in Energy and Combustion Science* **34**, 47–90. doi:10.1016/J.PECS.2006.12.001

Dietenberger MA, Boardman CR, Shotorban B, Mell W, Weise DR (2020) Thermal degradation modeling of live vegetation for fire dynamic simulator. In 'Proceedings, 2020 Spring Technical Meeting, Central States Section of the Combustion Institute', University of Alabama in Huntsville, AL. pp. 1–20. (University of Alabama in Huntsville, AL) Available at https://www.fs.usda.gov/treesearch/pubs/60852.

Dimitrakopoulos AP (2001*a*) A statistical classification of Mediterranean species based on their flammability components. *International Journal of Wildland Fire* **10**, 113–118. doi:10.1071/WF01004

Dimitrakopoulos AP (2001*b*) Thermogravimetric analysis of Mediterranean plant species. *Journal of Analytical and Applied Pyrolysis* **60**, 123–130. doi:10.1016/S0165-2370(00)00164-9

DiNenno PJ, Drysdale D, Beyler CL, Walton WD, Custer RLP, Hall JR Jr, Watts JM Jr (Eds) (2002) 'SFPE handbook of fire protection engineering.' (National Fire Protection Association and Society of Fire Protection Engineers: Quincy, MA)

Egozcue JJ, Pawlowsky-Glahn V (2005) Groups of parts and their balances in compositional data analysis. *Mathematical Geology* **37**, 795–828. doi:10.1007/S11004-005-7381-9

Egozcue JJ, Pawlowsky-Glahn V, Mateu-Figueras G, Barceló-Vidal C (2003) Isometric logratio transformations for compositional data analysis. *Mathematical Geology* **35**, 279–300. doi:10.1023/A:1023818214614

Egozcue JJ, Lovell D, Pawlowsky-Glahn V (2014) Testing compositional association. In 'Proceedings of the 5th International Workshop on Compositional Data Analysis, Vorau, Austria'. (Eds K Hron, P Filzmoser, M Templ). pp. 28–36. (Vorau, Austria) Available at http://www.statistik.tuwien.ac.at/CoDaWork/CoDaWork2013Proceedings.pdf.

Egozcue JJ, Pawlowsky-Glahn V, Gloor GB (2018) Linear association in compositional data analysis. *Austrian Journal of Statistics* **47**, 3–31. doi:10.17713/AJS.V47I1.689

Ehleringer JR, Cerling TE (1995) Atmospheric CO2 and the ratio of intercellular to ambient CO2 concentrations in plants. *Tree Physiology* **15**, 105–111. doi:10.1093/TREEPHYS/15.2.105

Fagbemi L, Khezami L, Capart R (2001) Pyrolysis products from different biomasses. *Applied Energy* **69**, 293–306. doi:10.1016/S0306-2619(01)00013-7

Ferguson SC, Dahale A, Shotorban B, Mahalingam S, Weise DR (2013) The role of moisture on combustion of pyrolysis gases in wildland fires. *Combustion Science and Technology* **185**, 435–453. doi:10.1080/00102202.2012.726666

Filzmoser P, Hron K, Templ M (2018) 'Applied compositional data analysis: with worked examples in R.' (Springer: Berlin)

Gibergans-Baguena J, Hervada-Sala C, Jarauta-Bragulat E (2020) The quality of urban air in Barcelona: a new approach applying compositional data analysis methods. *Emerging Science Journal* **4**, 113–121. doi:10.28991/ESJ-2020-01215

Goelz J (2001) Systematic experimental designs for mixed species plantings. *Native Plants Journal* **2**, 90–96. doi:10.3368/NPJ.2.2.90

Hardy CC (2005) Wildland fire hazard and risk: Problems, definitions, and context. *Forest Ecology and Management* **211**, 73–82. doi:10.1016/J.FORECO.2005.01.029

Hough WA (1969) Caloric value of some forest fuels of the southern United States. USDA Forest Service, Southeastern Forest Experiment Station, Research Note SE-120. (Asheville, NC) Available at http://www.treesearch.fs.fed.us/pubs/2778

Jarauta-Bragulat E, Hervada-Sala C, Egozcue JJ (2016) Air Quality Index revisited from a compositional point of view. *Mathematical Geosciences* **48**, 581–593. doi:10.1007/S11004-015-9599-5

Jegers HE, Klein MT (1985) Primary and secondary lignin pyrolysis reaction pathways. *Industrial & Engineering Chemistry Process Design and Development* **24**, 173–183. doi:10.1021/I200028A030

Jolly WM, Hintz J, Linn RL, Kropp RC, Conrad ET, Parsons RA, Winterkamp J (2016) Seasonal variations in red pine (*Pinus resinosa*) and jack pine (*Pinus banksiana*) foliar physio-chemistry and their potential influence on stand-scale wildland fire behavior. *Forest Ecology and Management* **373**, 167–178. doi:10.1016/J.FORECO.2016.04.005

Jones D (1984) Use, misuse, and role of multiple-comparison procedures in ecological and agricultural entomology. *Environmental Entomology* **13**, 635–649. doi:10.1093/EE/13.3.635

Kim S, Chen J, Cheng T, Gindulyte A, He J, He S, Li Q, Shoemaker BA, Thiessen PA, Yu B, Zaslavsky L, Zhang J, Bolton EE (2019) PubChem 2019 update: improved access to chemical data. *Nucleic Acids Research* **47**, D1102–D1109. doi:10.1093/NAR/GKY1033

Kynčlová P, Hron K, Filzmoser P (2017) Correlation between compositional parts based on symmetric balances. *Mathematical Geosciences* **49**, 777–796. doi:10.1007/S11004-016-9669-3

LeBlanc J, Uchimiya M, Ramakrishnan G, Castaldi MJ, Orlov A (2016) Across-phase biomass pyrolysis stoichiometry, energy balance, and product formation kinetics. *Energy & Fuels* **30**, 6537–6546. doi:10.1021/ACS.ENERGYFUELS.6B01376

Ledesma EB, Marsh ND, Sandrowitz AK, Wornat MJ (2002) An experimental study on the thermal decomposition of catechol. *Proceedings of the Combustion Institute* **29**, 2299–2306. doi:10.1016/S1540-7489(02)80280-2

Lenth R (2020) emmeans: Estimated Marginal Means, aka Least-Squares Means. Available at https://CRAN.R-project.org/package=emmeans

Liodakis S, Bakirtzis D, Dimitrakopoulos A (2002) Ignition characteristics of forest species in relation to thermal analysis data. *Thermochimica Acta* **390**, 83–91. doi:10.1016/S0040-6031(02)00077-1

Lovell AB, Brezinsky K, Glassman I (1989) The gas phase pyrolysis of phenol. *International Journal of Chemical Kinetics* **21**, 547–560. doi:10.1002/KIN.550210706

Lovell D, Pawlowsky-Glahn V, Egozcue JJ, Marguerat S, Bähler J (2015) Proportionality: a valid alternative to correlation for relative data. *PLoS Computational Biology* **11**, e1004075. doi:10.1371/JOURNAL.PCBI.1004075

Maleknia SD, Bell TL, Adams MA (2009*a*) Eucalypt smoke and wildfires: Temperature dependent emissions of biogenic volatile organic compounds. *International Journal of Mass Spectrometry* **279**, 126–133. doi:10.1016/J.IJMS.2008.10.027

Maleknia SD, Vail TM, Cody RB, Sparkman DO, Bell TL, Adams MA (2009*b*) Temperature-dependent release of volatile organic compounds of eucalypts by direct analysis in real time (DART) mass spectrometry: Temperature-dependent release of VOCs of eucalypts. *Rapid Communications in Mass Spectrometry* **23**, 2241–2246. doi:10.1002/RCM.4133

Mateu-Figueras G, Pawlowsky-Glahn V, Egozcue JJ (2013) The normal distribution in some constrained sample spaces. *SORT - Statistics and Operations Research Transactions* **37**, 29–56.

Matt FJ, Dietenberger MA, Weise DR (2020) Summative and ultimate analysis of live leaves from southern U.S. forest plants for use in fire modeling. *Energy & Fuels* **34**, 4703–4720. doi:10.1021/ACS.ENERGYFUELS.9B04107

May AA, McMeeking GR, Lee T, Taylor JW, Craven JS, Burling I, Sullivan AP, Akagi S, Collett JL, Flynn M, Coe H, Urbanski SP, Seinfeld JH, Yokelson RJ, Kreidenweis SM (2014) Aerosol emissions from prescribed fires in the United States: A synthesis of laboratory and aircraft measurements: Aerosols from US prescribed fires. *Journal of Geophysical Research, D, Atmospheres* **119**, 11,826–11,849. doi:10.1002/2014JD021848

McCarty RD, Hord J, Roder HM (1981) 'Selected properties of hydrogen (engineering design data)'. National Bureau of Standards, Monograph 168. (NBS: Boulder, CO)

McNaught AD, Wilkinson A, International Union of Pure and Applied Chemistry (Eds) (1997) 'Compendium of chemical terminology: IUPAC recommendations.' (Blackwell Science: Oxford)

Mell W, Maranghides A, McDermott R, Manzello SL (2009) Numerical simulation and experiments of burning douglas fir trees. *Combustion and Flame* **156**, 2023–2041. doi:10.1016/J.COMBUSTFLAME.2009.06.015

Montero-Serrano JC, Palarea-Albaladejo J, Martín-Fernández JA, Martínez-Santana M, Gutiérrez-Martín JV (2010) Sedimentary chemofacies characterization by means of multivariate analysis. *Sedimentary Geology* **228**, 218–228. doi:10.1016/J.SEDGEO.2010.04.013

Neves D, Thunman H, Matos A, Tarelho L, Gómez-Barea A (2011) Characterization and prediction of biomass pyrolysis products. *Progress in Energy and Combustion Science* **37**, 611–630. doi:10.1016/J.PECS.2011.01.001

Ni M, Leung DYC, Leung MKH, Sumathy K (2006) An overview of hydrogen production from biomass. *Fuel Processing Technology* **87**, 461–472. doi:10.1016/J.FUPROC.2005.11.003

Núñez-Regueira L, Rodríguez J, Proupín J, Mouriño B (1999) Design of forest biomass energetic maps as a tool to fight forest wildfires. *Thermochimica Acta* **328**, 111–120. doi:10.1016/S0040-6031(98)00631-5

Palarea-Albaladejo J, Martín-Fernández JA (2015) zCompositions — R package for multivariate imputation of left-censored data under a compositional approach. *Chemometrics and Intelligent Laboratory Systems* **143**, 85–96. doi:10.1016/J.CHEMOLAB.2015.02.019

Palarea-Albaladejo J, Martín-Fernández JA, Olea RA (2014) A bootstrap estimation scheme for chemical compositional data with nondetects. *Journal of Chemometrics* **28**, 585–599. doi:10.1002/CEM.2621

Pawlowsky-Glahn V, Egozcue JJ (2001) Geometric approach to statistical analysis on the simplex. *Stochastic Environmental Research and Risk Assessment* **15**, 384–398. doi:10.1007/S004770100077

Pawlowsky-Glahn V, Egozcue JJ, Tolosana-Delgado R (2015) 'Modelling and analysis of compositional data.' (Wiley: Chichester, UK)

Phillips MC, Myers TL, Johnson TJ, Weise DR (2020) In-situ measurement of pyrolysis and combustion gases from biomass burning using swept wavelength external cavity quantum cascade lasers. *Optics Express* **28**, 8680–8700. doi:10.1364/OE.386072

R Core Team (2020) 'R: A Language and Environment for Statistical Computing.' (R Foundation for Statistical Computing: Vienna, Austria) Available at https://www.R-project.org/

Reimann C, Filzmoser P, Hron K, Kynčlová P, Garrett RG (2017) A new method for correlation analysis of compositional (environmental) data – a worked example. *The Science of the Total Environment* **607–608**, 965–971. doi:10.1016/J.SCITOTENV.2017.06.063

Rogers JM, Susott RA, Kelsey RG (1986) Chemical composition of forest fuels affecting their thermal behavior. *Canadian Journal of Research* **16**, 721–726. doi:10.1139/X86-129

Romero B, Fernandez C, Lecareux C, Ormeño E, Ganteaume A (2019) How terpene content affects fuel flammability of wildland–urban interface vegetation. *International Journal of Wildland Fire* **28**, 614–627. doi:10.1071/WF18210

Ryan KC, Opperman TS (2013) LANDFIRE – A national vegetation/fuels data base for use in fuels treatment, restoration, and suppression planning. *Forest Ecology and Management* **294**, 208–216. doi:10.1016/J.FORECO.2012.11.003

Safdari M-S, Rahmati M, Amini E, Howarth JE, Berryhill JP, Dietenberger M, Weise DR, Fletcher TH (2018) Characterization of pyrolysis products from fast pyrolysis of live and dead vegetation native to the Southern United States. *Fuel* **229**, 151–166. doi:10.1016/J.FUEL.2018.04.166

Safdari M-S, Amini E, Weise DR, Fletcher TH (2019) Heating rate and temperature effects on pyrolysis products from live wildland fuels. *Fuel* **242**, 295–304. doi:10.1016/J.FUEL.2019.01.040

Safdari M-S, Amini E, Weise DR, Fletcher TH (2020) Comparison of pyrolysis of live wildland fuels heated by radiation vs. convection. *Fuel* **268**, 117342. doi:10.1016/J.FUEL.2020.117342

Scharko NK, Oeck AM, Myers TL, Tonkyn RG, Banach CA, Baker SP, Lincoln EN, Chong J, Corcoran BM, Burke GM, Ottmar RD, Restaino JC, Weise DR, Johnson TJ (2019*a*) Gas-phase pyrolysis products emitted by prescribed fires in pine forests with a shrub understory in the southeastern United States. *Atmospheric Chemistry and Physics* **19**, 9681–9698. doi:10.5194/ACP-19-9681-2019

Scharko NK, Oeck AM, Tonkyn RG, Baker SP, Lincoln EN, Chong J, Corcoran BM, Burke GM, Weise DR, Myers TL, Banach CA, Griffith DWT, Johnson TJ (2019*b*) Identification of gas-phase pyrolysis products in a prescribed fire: first detections using infrared spectroscopy for naphthalene, methyl nitrite, allene, acrolein and acetaldehyde. *Atmospheric Measurement Techniques* **12**, 763–776. doi:10.5194/AMT-12-763-2019

Sekimoto K, Koss AR, Gilman JB, Selimovic V, Coggon MM, Zarzana KJ, Yuan B, Lerner BM, Brown SS, Warneke C, Yokelson RJ, Roberts JM, de Gouw J (2018) High- and low-temperature pyrolysis profiles describe volatile organic compound emissions from western US wildfire fuels. *Atmospheric Chemistry and Physics* **18**, 9263–9281. doi:10.5194/ACP-18-9263-2018

Shafizadeh F (1982) Introduction to the pyrolysis of biomass. *Journal of Analytical and Applied Pyrolysis* **3**, 283–305. doi:10.1016/0165-2370(82)80017-X

Shafizadeh F (1984) The chemistry of pyrolysis and combustion. In 'The Chemistry of Solid Wood'. (Ed. R Rowell) Advances in chemistry. pp. 489–529. (American Chemical Society: Washington, D.C.) doi:10.1021/BA-1984-0207.CH013

Shafizadeh F, Fu YL (1973) Pyrolysis of cellulose. *Carbohydrate Research* **29**, 113–122. doi:10.1016/S0008-6215(00)82074-1

Shotorban B, Yashwanth BL, Mahalingam S, Haring DJ (2018) An investigation of pyrolysis and ignition of moist leaf-like fuel subject to convective heating. *Combustion and Flame* **190**, 25–35. doi:10.1016/J.COMBUSTFLAME.2017.11.008

Speranza A, Caggiano R, Pavese G, Summa V (2018) The study of characteristic environmental sites affected by diverse sources of mineral matter using compositional data analysis. *Condensed Matter* **3**, 16. doi:10.3390/CONDMAT3020016

Susott RA (1982) Characterization of the thermal properties of forest fuels by combustible gas analysis. *Forest Science* **28**, 404–420.

Tachajapong W, Lozano J, Mahalingam S, Zhou X, Weise DR (2008) An investigation of crown fuel bulk density effects on the dynamics of crown fire initiation in shrublands. *Combustion Science and Technology* **180**, 593–615. doi:10.1080/00102200701838800

Templ M, Hron K, Filzmoser P (2011) robCompositions: An R-package for robust statistical analysis of compositional data. In 'Compositional Data Analysis'. (Eds V Pawlowsky-Glahn, A Buccianti) pp. 341–355. (John Wiley & Sons, Ltd: Chichester, UK) doi:10.1002/9781119976462.CH25

Thió-Henestrosa S, Comas M (2016) CoDaPack v2 User's Guide. Available at http://ima.udg.edu/codapack/assets/codapack-manual.pdf

Thomas S, Ledesma EB, Wornat MJ (2007) The effects of oxygen on the yields of the thermal decomposition products of catechol under pyrolysis and fuel-rich oxidation conditions. *Fuel* **86**, 2581–2595. doi:10.1016/J.FUEL.2007.02.003

Tree DR, Tobiasson JR, Egbert SC, Adams BR (2019) Measurement of radiative gas and particle emissions in biomass flames. *Proceedings of the Combustion Institute* **37**, 4337–4344. doi:10.1016/J.PROCI.2018.06.221

Urbanski SP, Hao WM, Baker S (2008) Chemical Composition of Wildland Fire Emissions. In 'Wildland Fires and Air Pollution'. (Eds A Bytnerowicz, MJ Arbaugh, AR Riebau, C Andersen) Developments in Environmental Science. pp. 79–107. (Elsevier: Amsterdam, The Netherlands). doi:10.1016/S1474-8177(08)00004-1

USDA (2020) The PLANTS Database. National Plant Data Team, Greensboro, NC 27401–4901, USA. Available at http://plants.usda.gov

van den Boogaart KG, Tolosana-Delgado R (2013) 'Analyzing compositional data with R.' (Springer: Heidelberg)

Ward DE (2001) Combustion chemistry and smoke. In 'Forest Fires: Behavior and Ecological Effects'. (Eds EA Johnson, K Miyanishi) pp. 55–77. (Academic Press: San Diego, CA).

Ward DE, Hao WM (1991) Projections of emissions from burning of biomass for use in studies of global climate and atmospheric chemistry. Paper 91-128.4. Presented at the 84th Annual Meeting and Exhibition; Vancouver, British Columbia; June 16-21, 1991. (Air and Waste Management Association: Vancouver, British Columbia, Canada). Available at http://www.treesearch.fs.fed.us/pubs/43258

Ward DE, Radke LF (1993) Emissions measurement from vegetation fires: a comparative evaluation of methods and results. In 'Fire in the environment: the ecological, atmospheric, and climatic importance of vegetation fires: report of the Dahlem Workshop, held in Berlin, 15–20 March 1992'. (Eds PJ Crutzen, JG Goldammer) pp. 53–76. (John Wiley & Sons Ltd.).

Ward DE, Clements HB, Nelson RM Jr (1980) Particulate matter emission factor modeling for fire in southeastern fuels. In 'Sixth Conference on Fire and Forest Meteorology, Seattle, WA'. (Ed. RE Martin) pp. 276–284. (American Meteorological Society: Seattle, WA)

Weise DR, Fletcher TH, Johnson TJ, Hao WM, Dietenberger M, Princevac M, Butler B, McAllister S, O'Brien J, Loudermilk L, Ottmar R, Hudak A, Kato A, Shotorban B, Mahalingam S, Mell WE (2018) A project to measure and model pyrolysis to improve prediction of prescribed fire behavior. In 'Advances in Forest Fire Research 2018'. (Ed. DX Viegas) pp. 308–318. (Coimbra University Press: Coimbra, Portugal)

Weise DR, Jung H, Palarea-Albaladejo J, Cocker DR (2020*a*) Compositional data analysis of smoke emissions from debris piles with low-density polyethylene. *Journal of the Air & Waste Management Association* **70**, 834–845. doi:10.1080/10962247.2020.1784309

Weise DR, Palarea-Albaladejo J, Johnson TJ, Jung H (2020*b*) Analyzing wildland fire smoke emissions data using compositional data techniques. *Journal of Geophysical Research: Atmospheres* **125**, e2019JD032128. doi:10.1029/2019JD032128

Williams DR (2020) Earth Fact Sheet. Available at https://nssdc.gsfc.nasa.gov/planetary/factsheet/earthfact.html

Yashwanth BL, Shotorban B, Mahalingam S, Lautenberger CW, Weise DR (2016) A numerical investigation of the influence of radiation and moisture content on pyrolysis and ignition of a leaf-like fuel element. *Combustion and Flame* **163**, 301–316. doi:10.1016/J.COMBUSTFLAME.2015.10.006

Yokelson RJ, Susott R, Ward DE, Reardon J, Griffith DWT (1997) Emissions from smoldering combustion of biomass measured by open-path Fourier transform infrared spectroscopy. *Journal of Geophysical Research, D, Atmospheres* **102**, 18865–18877. doi:10.1029/97JD00852

Zhang Z, Zhang H, Zhou D (2011) Flammability characterisation of grassland species of Songhua Jiang-Nen Jiang Plain (China) using thermal analysis. *Fire Safety Journal* **46**, 283–288. doi:10.1016/J.FIRESAF.2011.03.004

*International Journal of Wildland Fire*
doi: 10.1071/WF20126_AC


**SUPPLEMENTARY MATERIAL**

# Application of compositional data analysis to determine the effects of heating mode, moisture status and plant species on pyrolysates

*David R. Weise[A,D], Thomas H. Fletcher[B], Mohammad-Saeed Safdari[B], Elham Amini[B] and Javier Palarea-Albaladejo[C]*
[A]USDA Forest Service, Pacific Southwest Research Station, Riverside, CA 92507, USA.
[B]Department of Chemical Engineering, Brigham Young University, Provo, UT 84602, USA.
[C]Biomathematics and Statistics Scotland, EH9 3FD Edinburgh, Scotland, UK.
[D]Corresponding author. Email: david.weise@usda.gov

Supplemental figures.

Average effect of plant species on pyrolysis gas composition expressed as deviation in log-ratio scale from the overall geometric mean. Values below zero represent average mole fractions lower than overall value while values above zero represent the opposite. Note that the plotted values are the average deviation of the estimated effect.

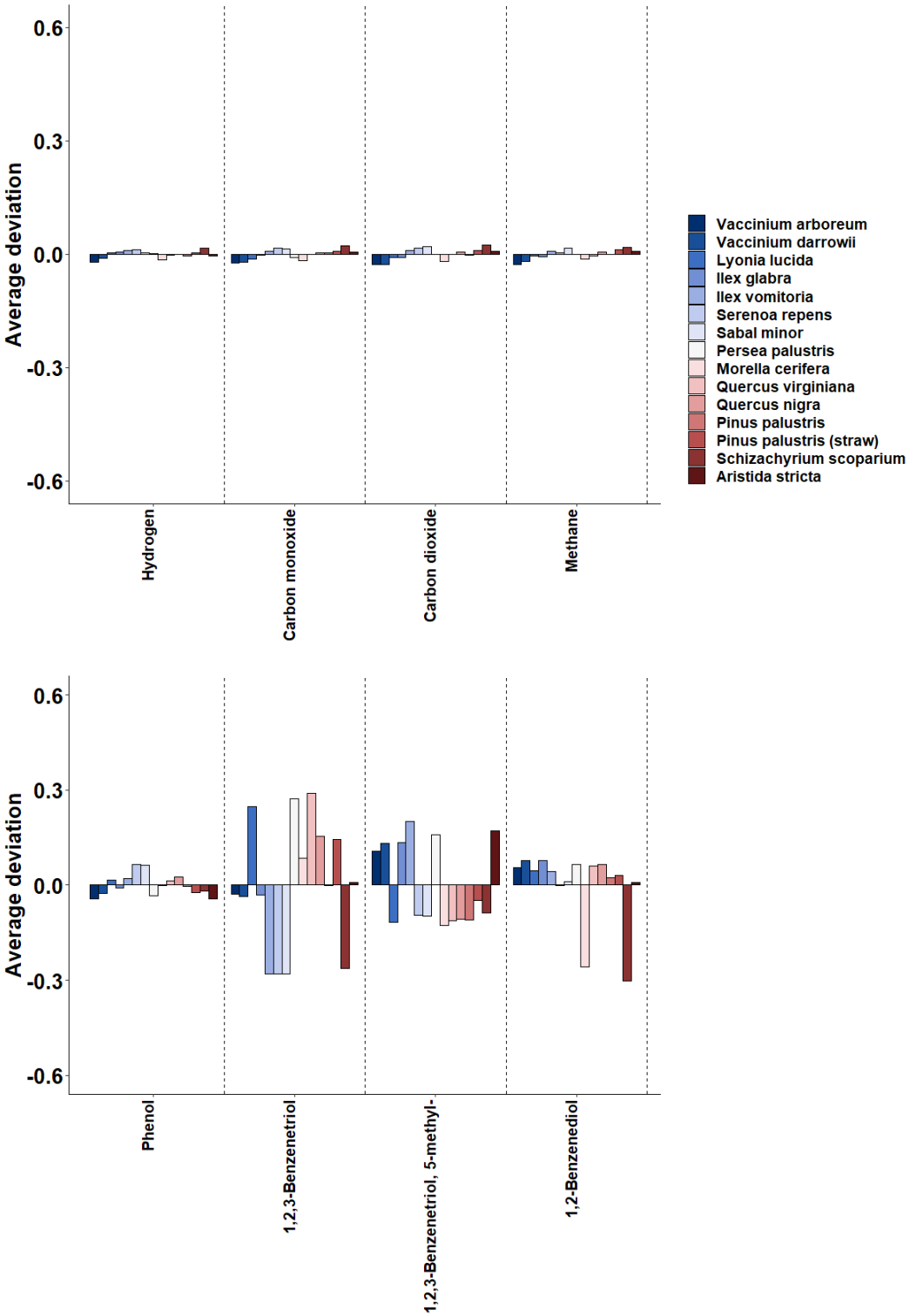
Average deviation
0.6
0.3
0.0
-0.3
-0.6
Hydrogen
Carbon monoxide
Carbon dioxide
Methane
Vaccinium arboreum
Vaccinium darrowii
Lyonia lucida
Ilex glabra
Ilex vomitoria
Serenoa repens
Sabal minor
Persea palustris
Morella cerifera
Quercus virginiana
Quercus nigra
Pinus palustris
Pinus palustris (straw)
Schizachyrium scoparium
Aristida stricta
Average deviation
0.6
0.3
0.0
-0.3
-0.6
Phenol
1,2,3-Benzenetriol
1,2,3-Benzenetriol, 5-methyl-
1,2-Benzenediol

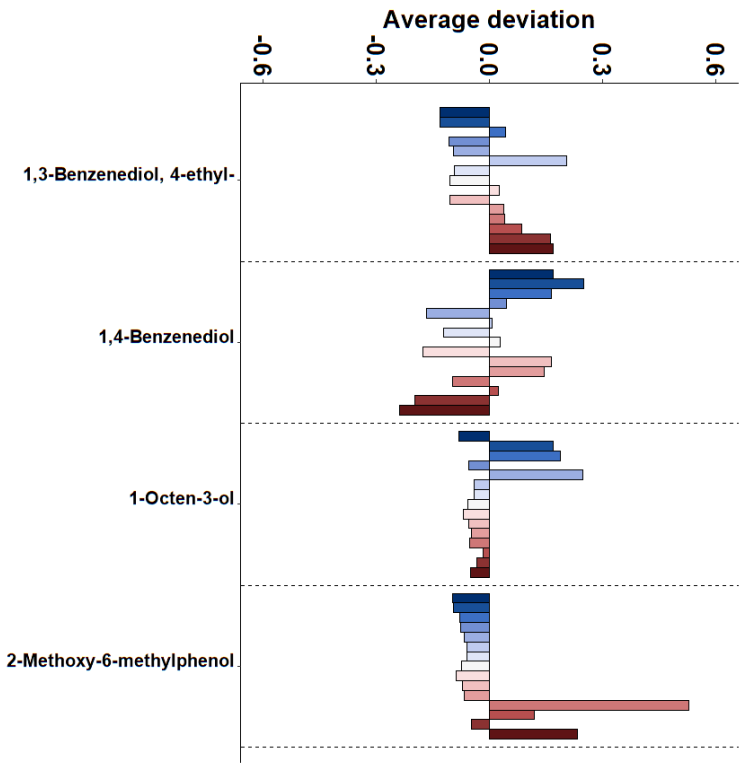
Average deviation
-0.6
-0.3
0.0
0.3
0.6
1,3-Benzenediol, 4-ethyl-
1,4-Benzenediol
1-Octen-3-ol
2-Methoxy-6-methylphenol

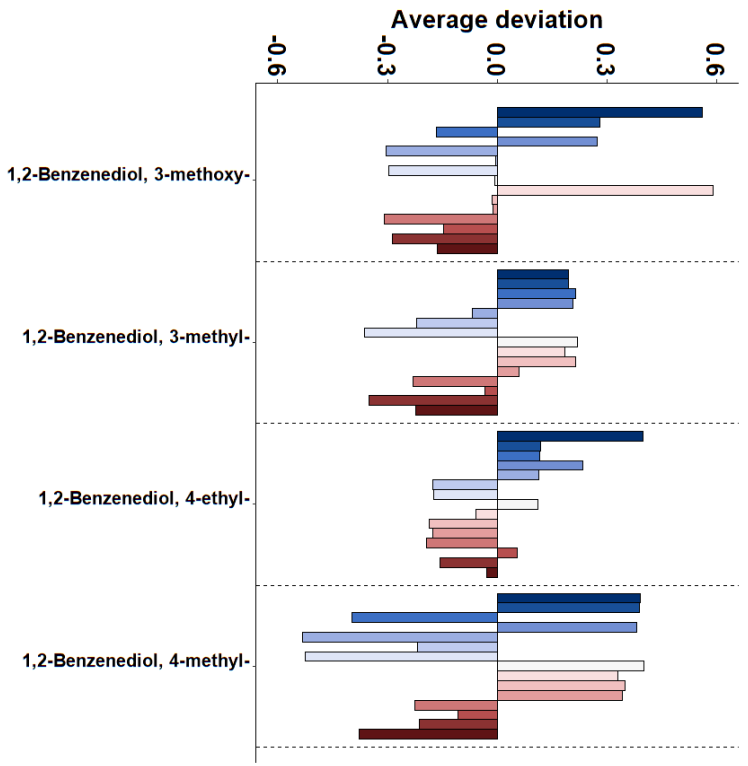
Average deviation
-0.6
-0.3
0.0
0.3
0.6
1,2-Benzenediol, 3-methoxy-
1,2-Benzenediol, 3-methyl-
1,2-Benzenediol, 4-ethyl-
1,2-Benzenediol, 4-methyl-

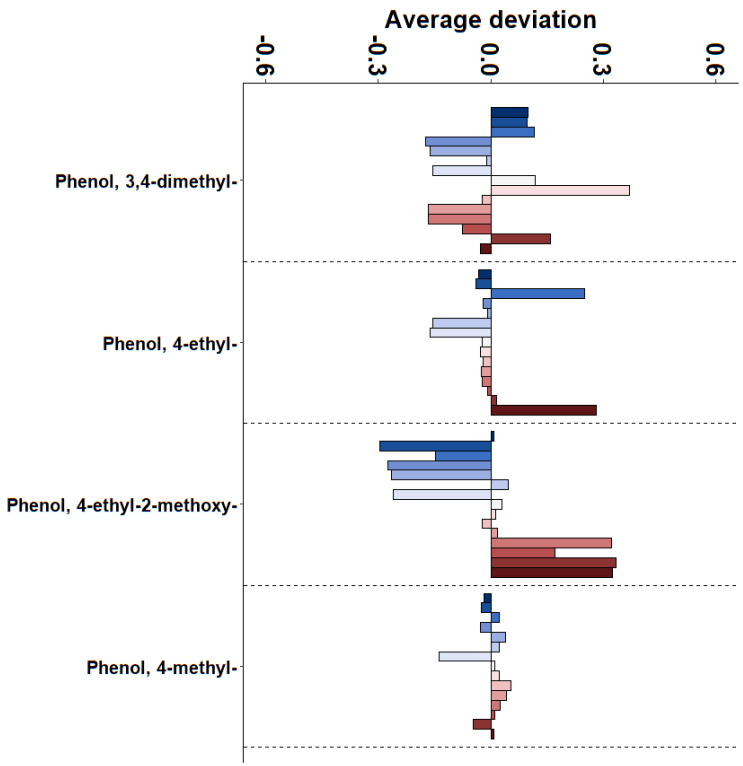
Average deviation
-0.6
-0.3
0.0
0.3
0.6
Phenol, 3,4-dimethyl-
Phenol, 4-ethyl-
Phenol, 4-ethyl-2-methoxy-
Phenol, 4-methyl-

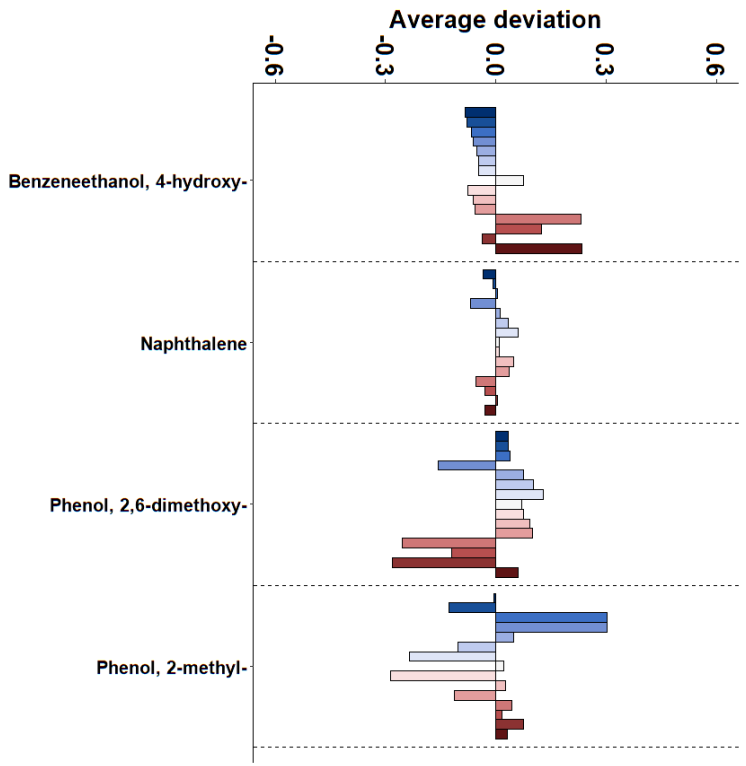
Average deviation
-0.6
-0.3
0.0
0.3
0.6
Benzeneethanol, 4-hydroxy-
Naphthalene
Phenol, 2,6-dimethoxy-
Phenol, 2-methyl-

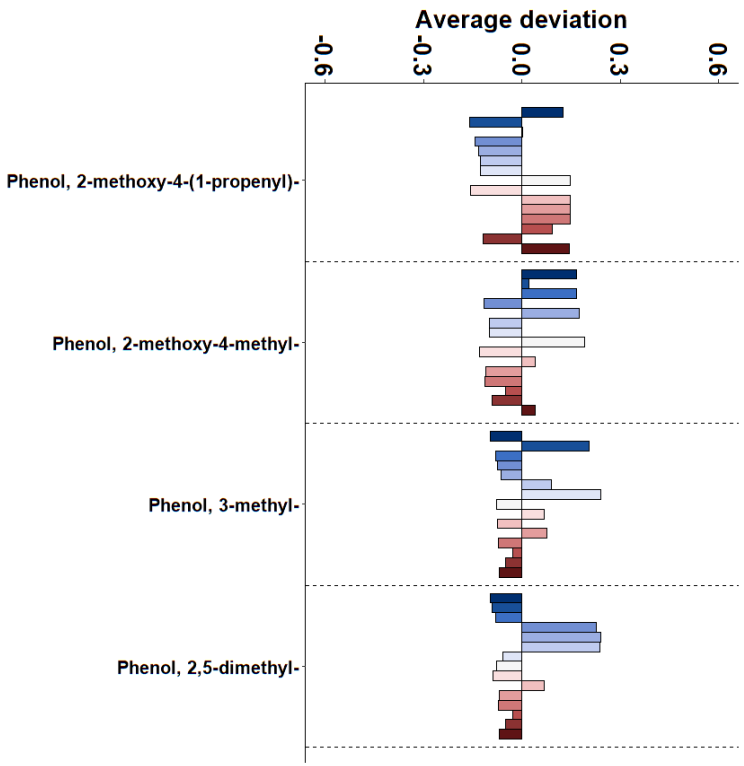
Average deviation
-0.6
-0.3
0.0
0.3
0.6
Phenol, 2-methoxy-4-(1-propenyl)-
Phenol, 2-methoxy-4-methyl-
Phenol, 3-methyl-
Phenol, 2,5-dimethyl-

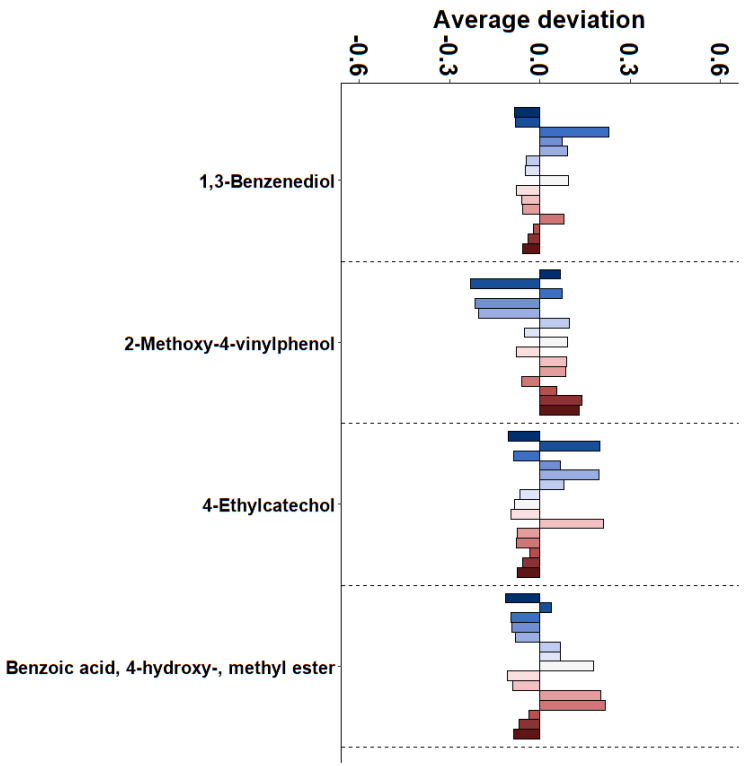
Average deviation
-0.6
-0.3
0.0
0.3
0.6
1,3-Benzenediol
2-Methoxy-4-vinylphenol
4-Ethylcatechol
Benzoic acid, 4-hydroxy-, methyl ester

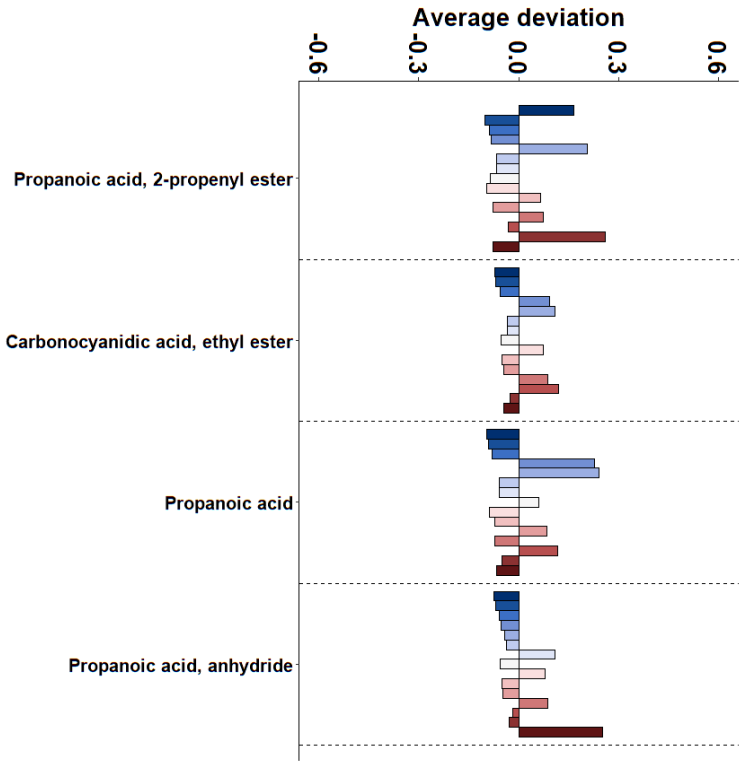
Average deviation
-0.6
-0.3
0.0
0.3
0.6
Propanoic acid, 2-propenyl ester
Carbonocyanidic acid, ethyl ester
Propanoic acid
Propanoic acid, anhydride

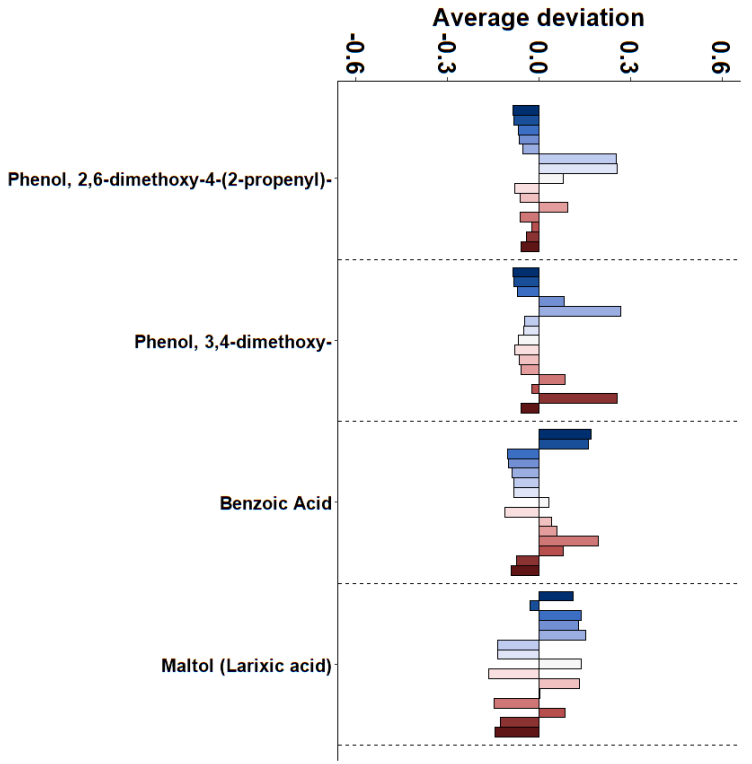
Average deviation
-0.6
-0.3
0.0
0.3
0.6
Phenol, 2,6-dimethoxy-4-(2-propenyl)-
Phenol, 3,4-dimethoxy-
Benzoic Acid
Maltol (Larixic acid)

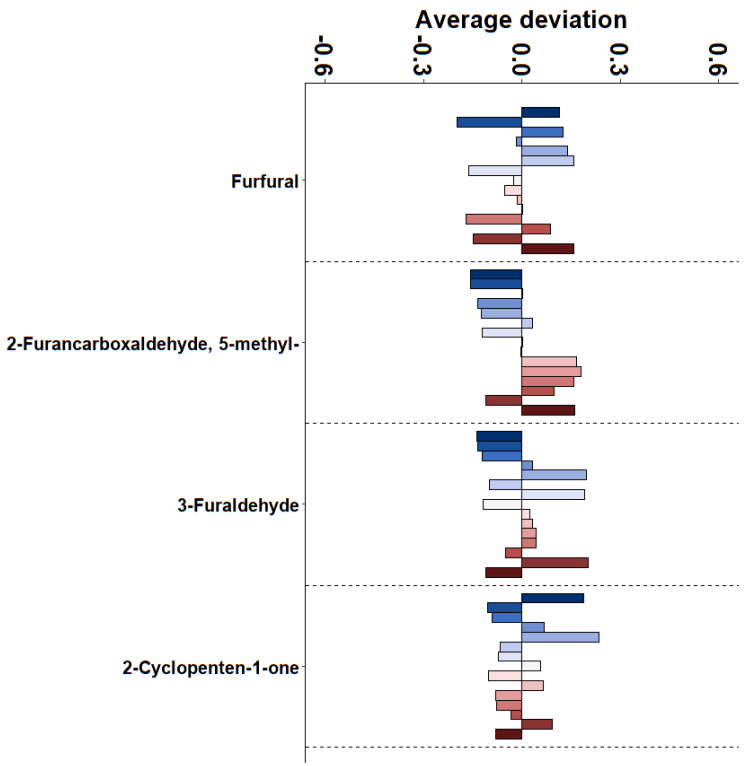
Average deviation
-0.6
-0.3
0.0
0.3
0.6
Furfural
2-Furancarboxaldehyde, 5-methyl-
3-Furaldehyde
2-Cyclopenten-1-one

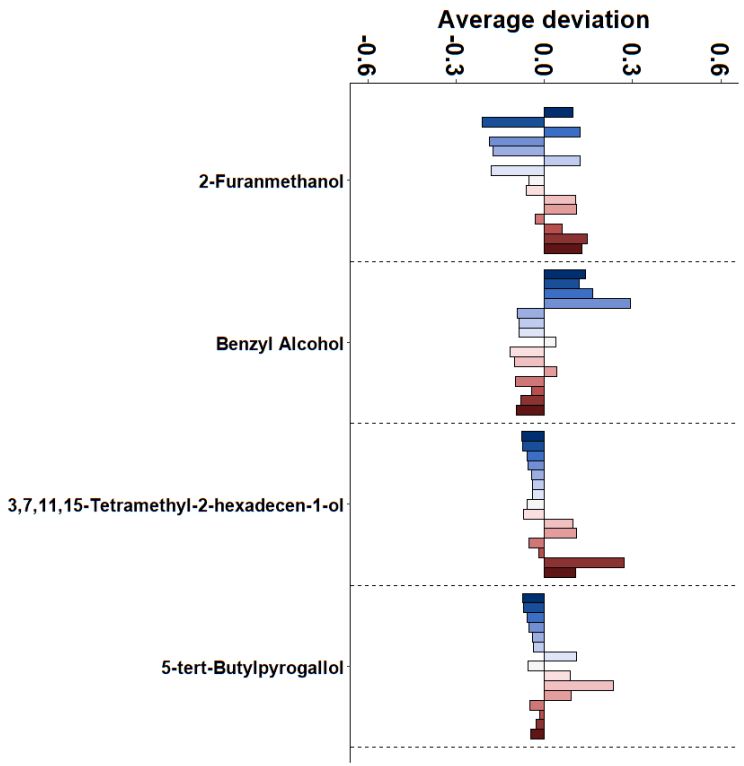
Average deviation
-0.6
-0.3
0.0
0.3
0.6
2-Furanmethanol
Benzyl Alcohol
3,7,11,15-Tetramethyl-2-hexadecen-1-ol
5-tert-Butylpyrogallol

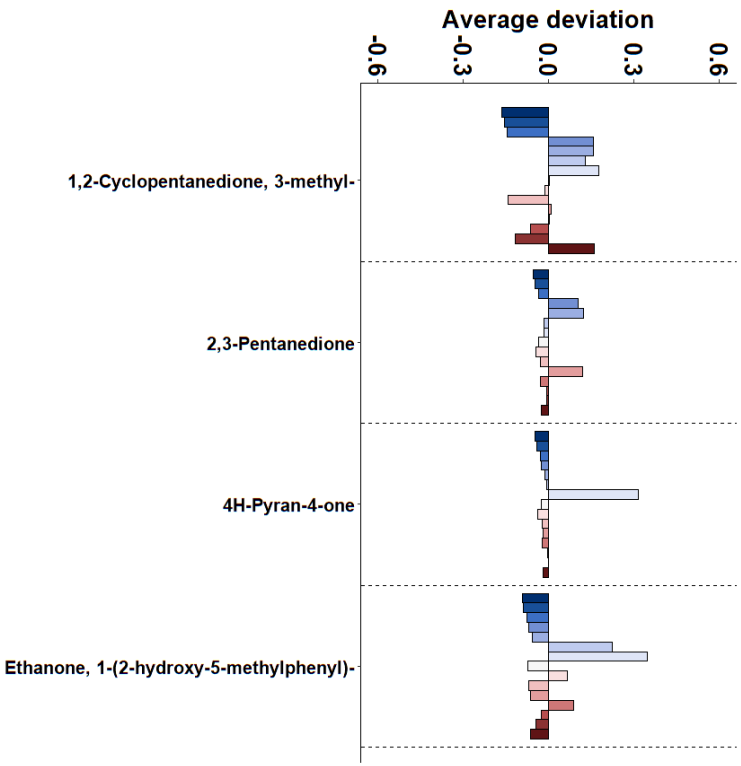
Average deviation
-0.6
-0.3
0.0
0.3
0.6
1,2-Cyclopentanedione, 3-methyl-
2,3-Pentanedione
4H-Pyran-4-one
Ethanone, 1-(2-hydroxy-5-methylphenyl)-

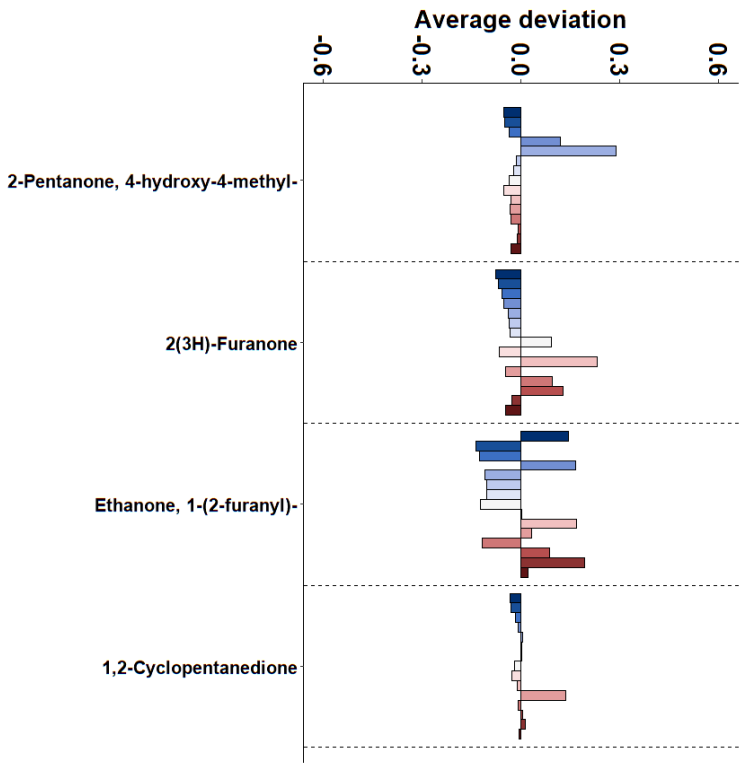
Average deviation
-0.6
-0.3
0.0
0.3
0.6
2-Pentanone, 4-hydroxy-4-methyl-
2(3H)-Furanone
Ethanone, 1-(2-furanyl)-
1,2-Cyclopentanedione

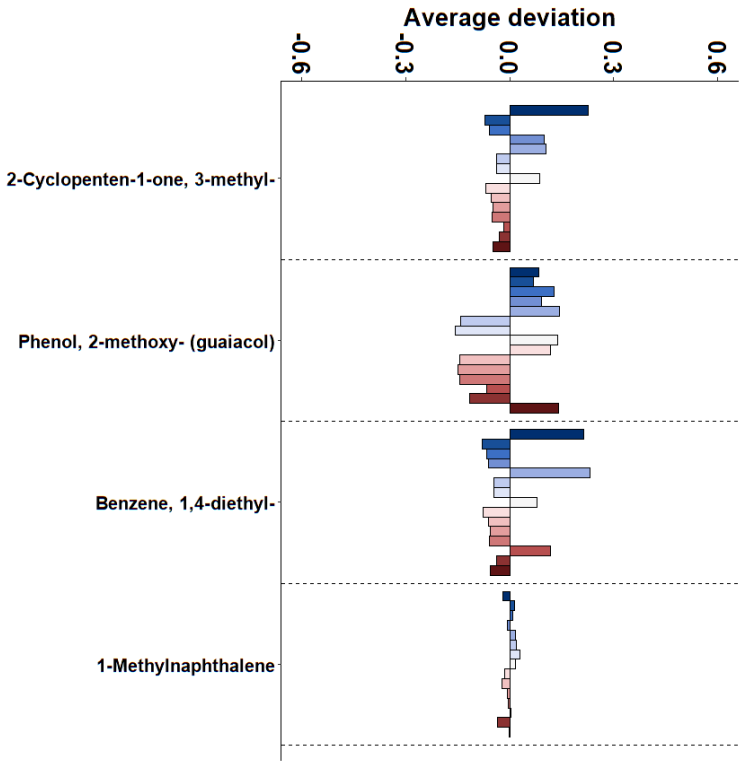
Average deviation
-0.6
-0.3
0.0
0.3
0.6
2-Cyclopenten-1-one, 3-methyl-
Phenol, 2-methoxy- (guaiacol)
Benzene, 1,4-diethyl-
1-Methylnaphthalene

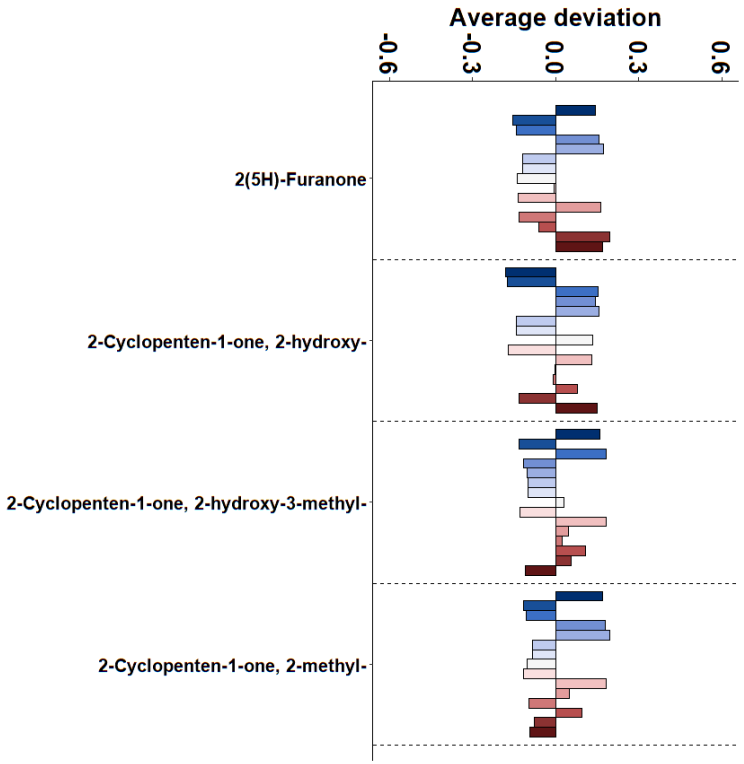
Average deviation
-0.6
-0.3
0.0
0.3
0.6
2(5H)-Furanone
2-Cyclopenten-1-one, 2-hydroxy-
2-Cyclopenten-1-one, 2-hydroxy-3-methyl-
2-Cyclopenten-1-one, 2-methyl-

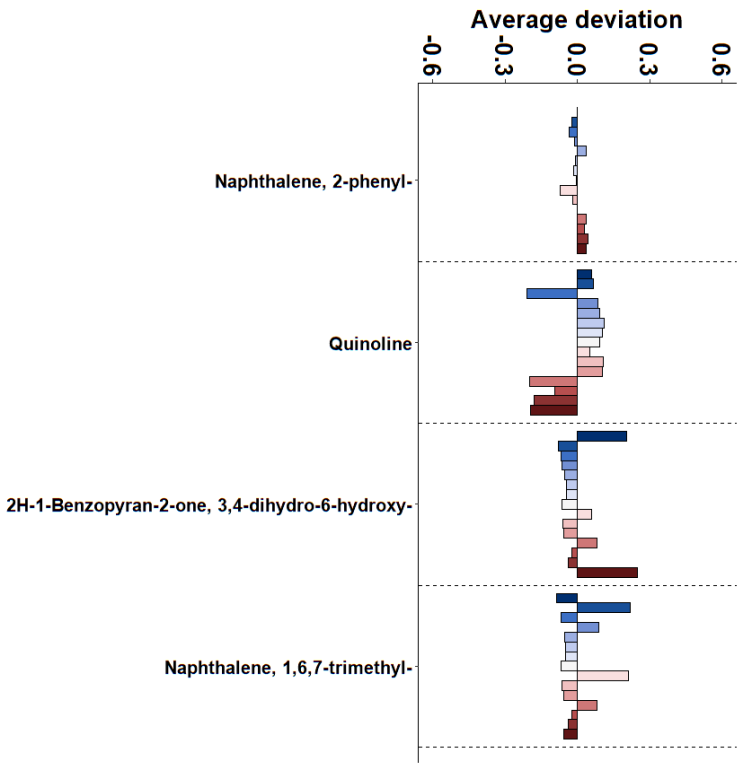
Average deviation
-0.6
-0.3
0.0
0.3
0.6
Naphthalene, 2-phenyl-
Quinoline
2H-1-Benzopyran-2-one, 3,4-dihydro-6-hydroxy-
Naphthalene, 1,6,7-trimethyl-

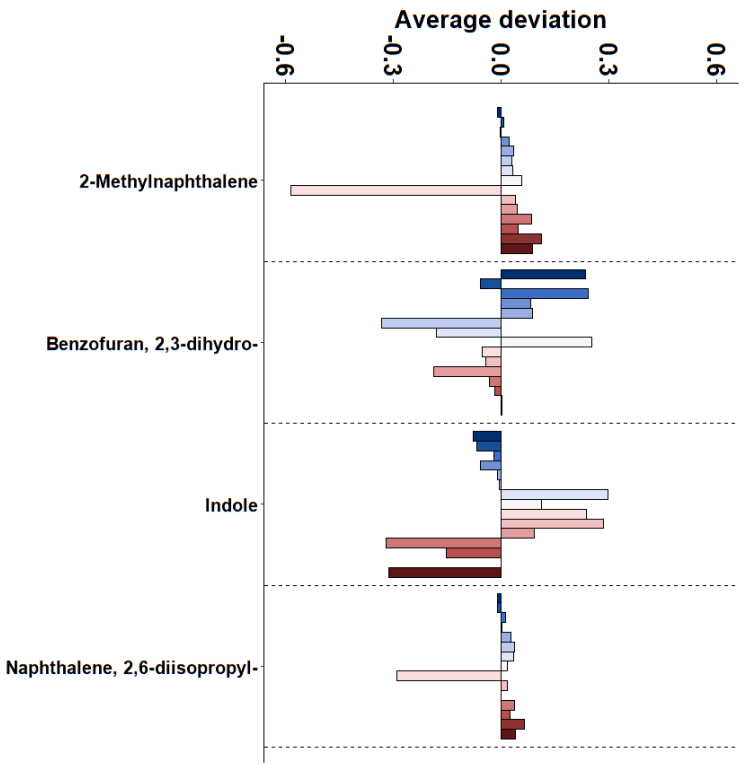
Average deviation
-0.6
-0.3
0.0
0.3
0.6
2-Methylnaphthalene
Benzofuran, 2,3-dihydro-
Indole
Naphthalene, 2,6-diisopropyl-

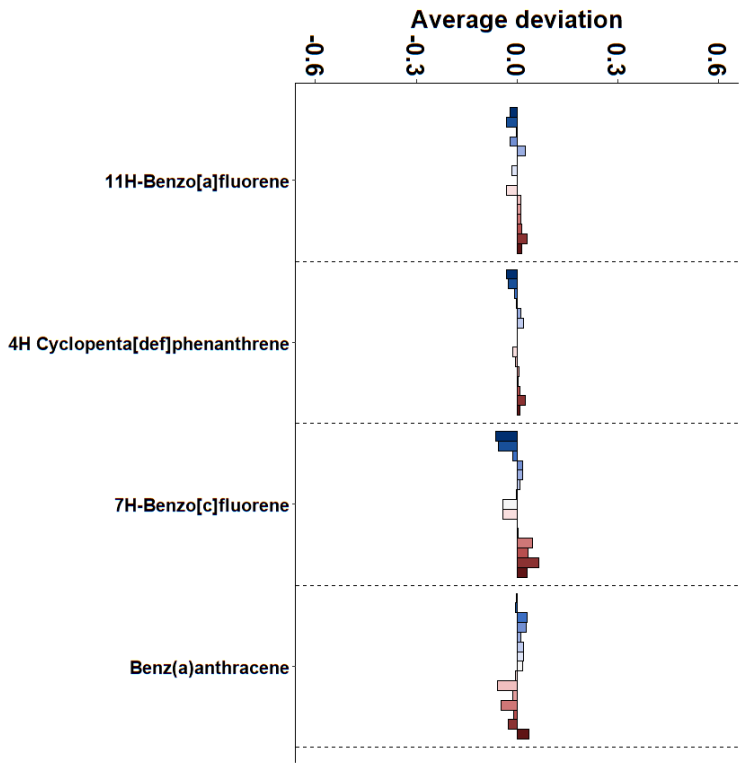
Average deviation
-0.6
-0.3
0.0
0.3
0.6
11H-Benzo[a]fluorene
4H Cyclopenta[def]phenanthrene
7H-Benzo[c]fluorene
Benz(a)anthracene

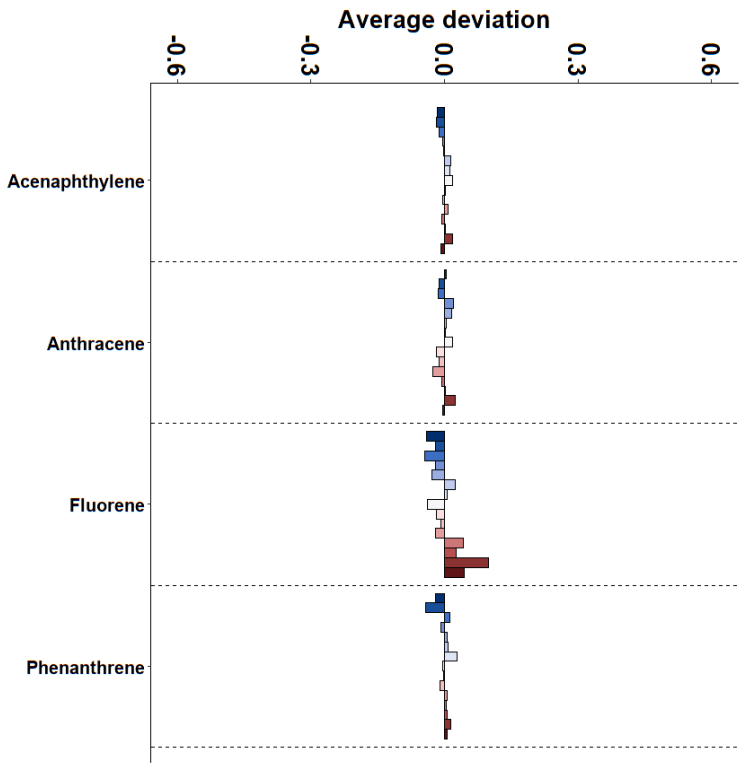
Average deviation
-0.6
-0.3
0.0
0.3
0.6
Acenaphthylene
Anthracene
Fluorene
Phenanthrene

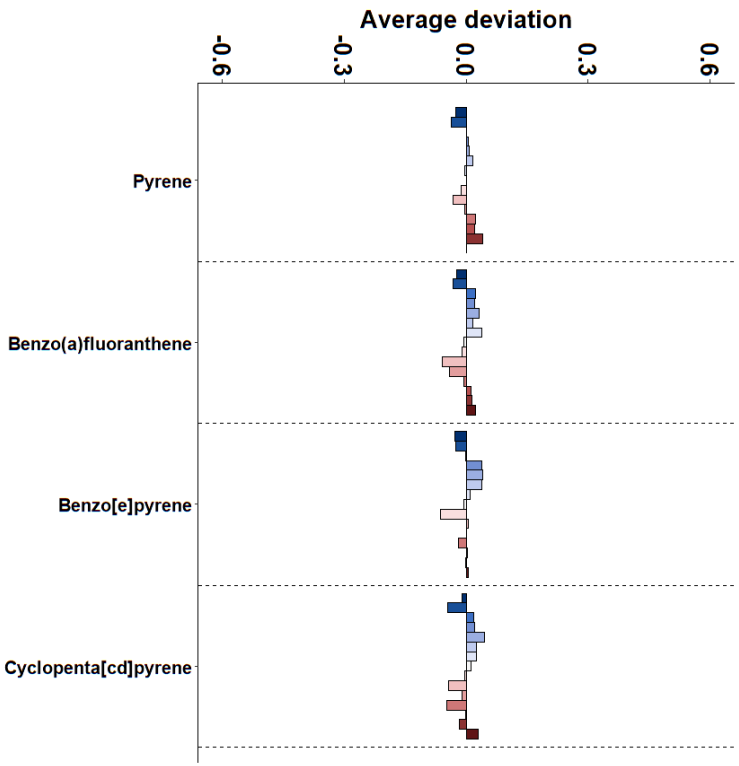
Average deviation
-0.6
-0.3
0.0
0.3
0.6
Pyrene
Benzo(a)fluoranthene
Benzo[e]pyrene
Cyclopenta[cd]pyrene

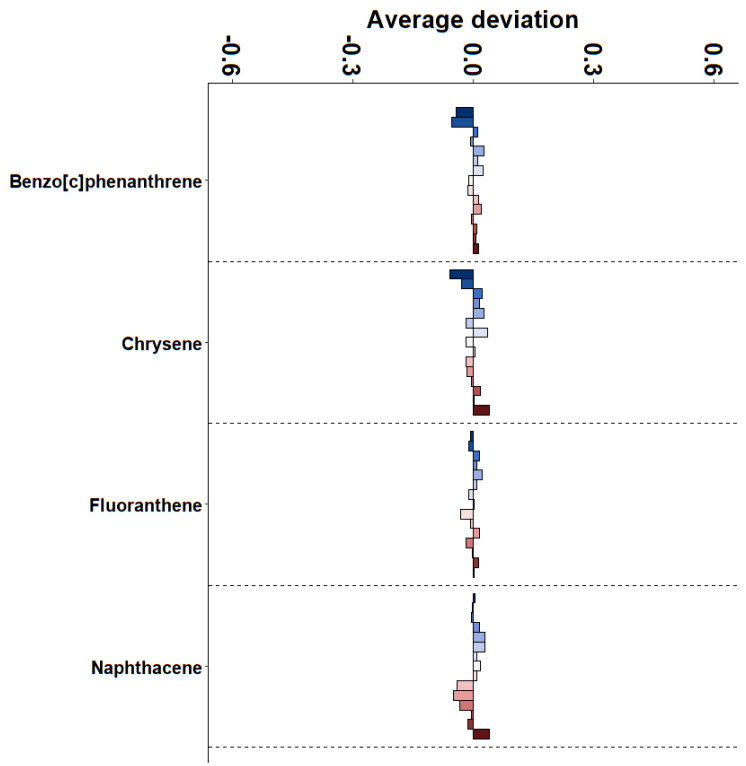
Average deviation
-0.6
-0.3
0.0
0.3
0.6
Benzo[c]phenanthrene
Chrysene
Fluoranthene
Naphthacene